Title:

Pathogen invasion-dependent tissue reservoirs and plasmid-encoded antibiotic degradation promote within-host plasmid transfer

Authors:

Erik Bakkeren[1,2,3*], Joana A. Herter[1], Jana S. Huisman[4,5], Ersin Gül[1], Alexander O. Brachmann[1], Jörn Piel[1], Roland R. Regoes[4], Sebastian Bonhoeffer[4], Médéric Diard[6,7], Wolf-Dietrich Hardt[1*]

Affiliations:

[1]Institute of Microbiology, Department of Biology, ETH Zurich, Zurich, Switzerland
[2]Present affiliation: Department of Zoology, University of Oxford, Oxford, UK
[3]Present affiliation: Department of Biochemistry, University of Oxford, Oxford, UK
[4]Institute of Integrative Biology, Department of Environmental Systems Science, ETH Zurich, Zurich, Switzerland
[5]Swiss Institute of Bioinformatics, Lausanne, Switzerland
[6]Biozentrum, University of Basel, Basel, Switzerland
[7]Botnar Research Centre for Child Health, Basel, Switzerland

*for correspondence:
hardt@micro.biol.ethz.ch
erik.bakkeren@zoo.ox.ac.uk

Key words:

Plasmids, Salmonella, Antibiotic resistance, tissue reservoirs, persistence

Abstract:

Many plasmids encode antibiotic resistance genes. Through conjugation, such plasmids can rapidly disseminate between bacterial strains. Previous work has identified gut-luminal donor/recipient blooms and tissue-lodged plasmid-bearing persister cells of the enteric pathogen *Salmonella enterica* serovar Typhimurium (*S.*Tm) that survive antibiotic-therapy in host tissues, as factors promoting plasmid dissemination among *Enterobacteriaceae*. However, the buildup of tissue reservoirs and their contribution to plasmid spread await experimental demonstration. Here, we asked if reseeding-acquisition-invasion cycles by *S.*Tm could serve to diversify tissue-lodged plasmid reservoirs, and thereby promote plasmid spread. Starting with intraperitoneal mouse infections, we demonstrate that *S.*Tm reseeding the gut lumen from either growing populations or persisters initiates clonal expansion. ESBL plasmid-encoded gut luminal antibiotic degradation by donors can foster recipient survival under beta-lactam antibiotic treatment, enhancing transconjugant formation upon reseeding. *S.*Tm transconjugants can subsequently re-enter host tissues introducing the new plasmid into the tissue-lodged reservoir. Population dynamics analyses pinpoint recipient migration into the gut lumen as rate-limiting for plasmid transfer dynamics in our model. Priority effects may limit reservoir formation in host tissues. Once transconjugant reservoirs are formed, persisters and chronically infecting transconjugant populations may serve complementary functions. The former are more numerous and may be more efficient vehicles promoting plasmid spread, while persister subpopulations guarantee plasmid reservoir maintenance even if the reservoir lacks appropriate resistance genes. Overall, our proof of principle data indicates that luminal antibiotic degradation and shuttling between the gut lumen and tissue-resident reservoirs can promote the accumulation and spread of plasmids within a host over time.

Main text:

Introduction:

The accumulation of antibiotic resistance genes in pathogenic bacterial strains is an important cause of antibiotic treatment failure. Conjugative antibiotic resistance plasmids are key drivers of this accumulation, accelerating the emergence of new bacterial strains genetically resistant to antibiotics (1). The mechanisms that contribute to the spread of resistance plasmids within an infected host are still not fully established.

Recently, we showed that the spread of plasmids within hosts can be aided by reservoirs of cells phenotypically recalcitrant to antibiotic therapy (2). This process is called persistence and refers to a property of bacterial populations in which one subpopulation is killed by an antibiotic parallel to another subpopulation that is killed slowly ("persisters"), defined by phenotypic and not genotypic properties (3, 4). Persisters can not only lead to antibiotic treatment failure, but they also have important implications for the evolution of antibiotic resistance (5-7) or virulence (8, 9), and serve as long term reservoirs promoting the spread of resistance plasmids. We showed this using the model organism *Salmonella enterica* serovar Typhimurium (*S.*Tm) (2). Invasive *S.*Tm cells form reservoirs of recalcitrant cells inside of host tissues (i.e., tissue persister reservoirs) that are difficult to treat with antibiotics (2, 9-13). After treatment, these *S.*Tm cells can reseed the gut lumen from their reservoirs along with any plasmids they carry. In the gut lumen, this provides the plasmids with the opportunity to conjugate into new host bacteria. Thereby, plasmids can subvert persisters to ensure long-term association within a given host. Besides persisters, *S.*Tm tissue invasion also creates a susceptible subpopulation within the host tissues. In the absence of antibiotic therapy, the latter cells are generally more numerous than the persisters and are thought to drive chronic infections (12-15). Moreover, these cells are known to re-seed the gut lumen over time (16). However, the role of this second tissue-lodged pathogen population in plasmid dissemination remained to be formally established.

Although very specific characteristics define antibiotic persistence (i.e., biphasic killing curves defining the susceptible and tolerant subpopulations) (3), there are many similarities to persistent (aka long-term, chronic) infection. Numerous bacterial pathogens can survive or evade host immune defenses and antibiotics alike in a recalcitrant state (e.g. *Pseudomonas aeruginosa, Escherichia coli, Staphylococcus aureus,* or *Salmonella enterica*) (4, 8, 17). Using mouse models, tissue reservoirs of *S.*Tm antibiotic persisters located in the intestinal mucosa or systemic sites can reseed the gut lumen after the cessation of antibiotic therapy (2, 9, 12, 18, 19). In chronically infected hosts, the pathogen population tends to diversify forming non-growing and growing subpopulations which are kept in check by immune defenses, but can rise upon neutralization of cytokines (e.g. IFNγ or TNFα) (14, 20). During monoclonal infections characteristic of many experimental models, intraspecies priority effects from *S.*Tm colonizing a given site within the host reduce the chances of colonization by pathogen cells that are arriving later (16). However, gut colonization is rarely a monoclonal process. This has been demonstrated in longitudinal clinical studies monitoring fecal *Enterobacteriaceae* populations, but also shown in swine where different strains of *Salmonella* colonize the lymph nodes compared to the gut lumen (21-24). Based on these considerations, we hypothesized that repeated re-seeding and re-infection events during persistent infection may promote plasmid spread.

Finally, we reasoned that certain resistance plasmids should themselves expedite reseeding-transfer-invasion cycles within the infected host. In particular, this should pertain to plasmid-encoded resistance genes encoding enzymes degrading antibiotics with an extra-cytoplasmic target (e.g. beta-lactamases). Among these, the extended spectrum beta-lactamases (ESBL) capable of hydrolyzing a wide variety of beta-lactam antibiotics including ampicillin and cephalosporins, are of particular concern (25). These periplasmic enzymes may facilitate reseeding of sensitive recipients, as

resistance plasmids encoding beta-lactamases are able to reach high density under beta-lactam treatment, and clear the local environment from antibiotics, as shown *in vitro* (26). However, it had remained unclear if such donor-mediated reduction of local beta-lactam concentrations would suffice for promoting survival of susceptible recipients *in vivo*, fostering plasmid transfer and subsequent reservoir formation in the host's tissue.

To address this, we quantitatively assessed the link between within-host plasmid transfer, invasion-reservoir formation-reseeding cycles and plasmid accumulation in the host's tissues using *S.*Tm mouse models for both antibiotic persistence and chronic infection. To study these processes in a proof of concept approach, we chose donor-recipient-plasmid combinations featuring a high conjugation efficiency and relieved potential restrictions to conjugation or reservoir formation in the mouse gut like colonization resistance conferred by the microbiota, and priority effects of strains that already colonize tissue reservoirs. Thereby, we could demonstrate expansion of the plasmid diversity in the gut tissue reservoir, a role for the chronically infecting *S.*Tm subpopulation and the effect of gut luminal antibiotic degradation by beta-lactamase expressing donor strains.

Results:

Plasmids that enter *S.*Tm in the gut lumen can be stored in intestinal tissue reservoirs

To study plasmid transfer within a host and its subsequent storage in the host tissues, we modified a mouse model from our previous work (2). For most plasmid transfer experiments, we used the IncI1 plasmid P2 (a close relative of extended-spectrum beta-lactamase (ESBL) plasmids; also known as pCol1b9), which naturally occurs in *S.*Tm SL1344 and spreads in the gut of antibiotic pretreated mice and during diet-elicited *Enterobacteriaceae* blooms (2, 27-31).

For all experiments, we used streptomycin resistant derivatives of *S.*Tm ATCC 14028S that naturally do not contain P2 as recipient strains. We infected 129/SvEv mice intraperitoneally (i.p.) with recipients to allow the formation of tissue reservoirs of *S.*Tm (**Fig. 1A**; left side, green) (2). The advantage of this approach is three-fold. First, it allows us to study plasmid transfer and subsequent tissue storage in models for antibiotic persistence (the focus of (2)) and to extend the work to persistent infection (this work). This is attributable to the capacity of the *Nramp1*-positive 129/SvEv mice to limit systemic pathogen growth during chronic infections (14, 32). Second, i.p. infection bypasses the need for gut colonization, ensuring that plasmid transfer observed later in the experiment is truly a result of plasmid conjugation into recipients entering from tissue reservoirs into the gut lumen. Third, the i.p. infection model mimics tissue reservoirs that are established after systemic spread following gut colonization (and therefore allows us to study the role of persistent infection in plasmid transfer dynamics) (2, 14, 16, 33). We would like to point out one caveat of this i.p. model, in that it eliminates the contribution of priority effects attributable to the inoculation route. As natural infections would occur via the oral colonization route, sites that are normally occupied by invading *S.*Tm cells (e.g. the mesenteric lymph node; mLN) are less colonized after i.p. infection. This means that invasion events from the gut luminal side later in the experiment are likely over-estimated in this model. On the other hand, this provides us with an exquisitely sensitive system to ask if tissue re-invasion can in principle expand the plasmid reservoirs within a host.

Next, we treated mice with a dose of streptomycin to suppress the microbiota and allow colonization of $P2^{cat}$ carrying donor strains (Sm^R) introduced orally (**Fig. 1A**, blue). Note that both the donors and recipient strains used in this experimental model are streptomycin resistant. Therefore, the systemic infection by the recipients remains unaffected by the antibiotic (= persistent systemic infection model). We used a derivative of *S.*Tm SL1344 that lacks functional type 3 secretions systems (TTSS)-1 and -2 (*invG* and *ssaV* mutant; $SL1344^{Avir}$) (34). This prevented invasion of the *S.*Tm donors into tissues to exclude tissue-localized plasmid transfer. We used SL1344 derivatives to study

153 interspecies interactions, rather than isogenic strain interactions that would limit co-existence of
154 donors and recipients in the gut after reseeding (16, 35). Feces were monitored over time to
155 investigate plasmid transfer dynamics and mice were euthanized at day 10 post infection to assess
156 the formation of new intra-cellular plasmid reservoirs by recipients that had obtained a plasmid
157 (transconjugants; **Fig. 1A**, red).
158 One day after the addition of donors (SL1344^{Avir} P2^{cat}), recipients started reseeding into the
159 gut lumen and transconjugants were detected in the feces (**Fig. 1B, Fig. S1A**). By day 10 of the
160 experiment, transconjugants were detected in the majority of mice (8/13 mice; **Fig. 1B**). Reseeding
161 and plasmid acquisition depended on the TTSS-2 encoded on SPI-2, as recipients lacking a functional
162 TTSS-2 (14028S *ssaV* mutant; *S.*Tm^{SPI-2}) failed to reseed frequently, and consequently transconjugants
163 were rarely observed (1/8 mice; **Fig. 1B. Fig. S1B**). Their failure to establish substantial tissue
164 reservoir sizes (e.g. in the spleen, liver, or gall bladder) could explain the limited reseeding of *S.*Tm^{SPI-2}
165 (**Fig. 1C**). These results indicated that bacteria reseeding from tissue reservoirs can gain plasmids in
166 the gut. In contrast to previous work (2) this occurred without previous selection for persister sub-
167 populations. This allows us to assess the contribution of growing tissue-lodged pathogen
168 subpopulations. Importantly, we analyzed here if the gut luminal plasmid was carried back into host
169 tissues by transconjugants. Indeed, transconjugants were detected in the mLNs of mice where gut
170 luminal plasmid transfer was observed. Occasionally such transconjugants were also observed in
171 other tissue reservoirs such as the spleen and liver associated with further systemic spread after
172 tissue invasion (**Fig. 1C**).
173 Next, we tested if this process could be generalized to other donors colonizing the gut lumen.
174 For this, we used *E. coli* 536 carrying P2^{cat} as a donor. This strain is naturally streptomycin resistant
175 and colonizes the streptomycin-pretreated mouse gut for long periods of time (36, 37). Also in this
176 case, reseeding of *S.*Tm 14028S recipients occurred followed by the formation of transconjugants in
177 the majority of the mice (7/12 mice) (**Fig. 1D, Fig. S1C**). Once again, this was associated with the
178 formation of new plasmid tissue reservoirs by invading transconjugants, primarily in the mLN (**Fig.
179 1E**). To assess if this experimental model allowed the comparison between both persistent infection
180 and antibiotic persistence, we performed a control experiment in which we treated mice three times
181 with ceftriaxone 2 days after i.p. infection to select for persisters (**Fig. S2**), as done previously (2).
182 After the addition of *E. coli* 536 P2^{cat} donors, *S.*Tm^{WT} recipients began to reseed in some mice.
183 However, this occurred later and in a smaller number of the analyzed mice, as antibiotic persisters
184 are much less abundant (and need to re-enter growth) compared to the much larger population of
185 persistently infecting *S.*Tm^{WT} recipient cells. Regardless, this reseeding was also associated with
186 plasmid transfer and the occasional formation of tissue reservoirs of transconjugants in the mLN (**Fig.
187 S2**).
188 Altogether, this demonstrates that plasmids can subvert both *S.*Tm derived from tissue
189 lodged populations of antibiotic persisters, or from persistent infections. Cells from either type of
190 tissue lodged population can re-enter the gut lumen, and serve as recipients in interspecies
191 interactions. This process can be followed by reinvasion forming new tissue reservoirs, capturing a
192 record of conjugative plasmids that had previously been present in the gut lumen.
193
194 **Reseeding of the gut lumen, plasmid transfer, and the formation of new reservoirs is limited by the
195 gut luminal carrying capacity and the conjugation rate**
196
197 Next, we examined the dynamics of pathogen-assisted plasmid transfer and storage, and the
198 possible routes that recipients and transconjugants take to exit and re-enter host tissues in more
199 detail. First, we explored possible sources of persistently infecting recipients that reseed the gut
200 lumen by characterizing the localization of *S.*Tm in tissue reservoirs. We infected mice i.p. with *S.*Tm
201 14028S recipients and euthanized mice 2 days later, while keeping the gut luminal microbiota intact

202 (at the time point when normally the donors are added). As expected based on previous work (2, 14,
203 16, 38, 39), *S*.Tm were found in the spleen, liver, and kidney at high density (**Fig. S3**), which likely
204 occurred because of blood flow to these organs immediately after i.p. infection of *S*.Tm (39).
205 Although bacteria were not detected in the feces (our readout for reseeding), *S*.Tm was found in the
206 content of the small intestine (i.e. primarily the jejunum and ileum, but also the duodenum), and this
207 was correlated with *S*.Tm in the tissues of these sites (**Fig. S3**). Furthermore, we found high densities
208 of *S*.Tm in the lining of the small intestinal tissues that contains the gut-associated tissues such as
209 Peyer's patches (here called small intestinal gut associated lymphoid tissues; S.I. GALT). The gall
210 bladder contained some *S*.Tm, but the low densities suggest that the gall bladder is not the primary
211 route of reseeding in this model (as suggested in some experimental models (16)). Future work may
212 address if *S*.Tm reseeds from the small intestinal tissues after spread from blood or lymphatic supply.
213 Instead, we focused on the dynamics of reseeding followed by plasmid transfer into this
214 luminal pathogen population, and asked in which conditions this occurs. We mixed equal ratios of
215 recipient strains harbouring three different sequence-tagged barcodes at a neutral location in the
216 chromosome (14028S Sm^R *TAG1-3*; 1:1:1 ratio) and i.p. infected mice (same mice as in **Fig. 1B**). As
217 donor strains, we used $SL1344^{Avir}$ containing P2 labelled with four additional unique sequence tags
218 ($P2^{TAG4-7}$; 1:1:1:1 ratio). All tags can be identified using quantitative PCR (39). At the end of the
219 experiment, we analyzed the ratio of each of these tags in the recipient population (enriching for
220 recipients = recipients + transconjugants) by qPCR. To visually correlate reseeding of *S*.Tm into the
221 gut lumen with the localization of these tags in tissue reservoirs, we sorted and color-coded the tags
222 according to the most abundant tag in the feces. While chromosomal tags were evenly distributed in
223 primary tissue reservoirs (e.g. spleen and liver), the feces were typically dominated by just one of the
224 three tagged strains (**Fig. 2A, Fig. S4**). Thus, reseeding from these tissue reservoirs is a rare process
225 that is followed by clonal expansion. We also analyzed the gall bladder as a possible source of
226 reseeding, and the mLN as a site where new tissue reservoirs are formed after reinvasion of
227 reseeding *S*.Tm. Although the chromosomal tags were slightly more skewed in the gall bladder
228 compared to the spleen and liver, there was no correlation between the rank of the tags found in the
229 feces and in the gall bladder (**Fig. 2A, Fig. S4A**; e.g. mouse 7 contains different most abundant tags in
230 the feces and gall bladder). Interestingly, the mLN and the feces typically shared the same most
231 abundant chromosomal tag (~10-fold median reduction of the proportion of the most and second
232 most abundant tag in the feces; **Fig. 2A**), suggesting that reseeding followed by reinvasion could be
233 skewing this distribution. Note that the mLN population likely reflects the population that has
234 invaded into the gut tissue. However, due to unavoidable background contamination from separating
235 the gut tissue from the gut lumen, we chose to examine the mLN instead. This correlation between
236 mLN and fecal chromosomal tags was not seen in one mouse (mouse 9 in **Fig. S4**), in which recipients
237 were not found at high densities in the feces, further supporting this hypothesis. We plotted the
238 plasmid tags found in the transconjugant population in the same manner (**Fig. 2B**). In mice where
239 plasmid transfer was detected (population sizes in **Fig. S1A**; raw tag data in **Fig. S4**), almost all
240 plasmid tags were found, although their distribution was skewed (**Fig. 2B**). Importantly, the plasmid
241 tags found in the feces were mostly also found in the mLN, implying that plasmids were carried into
242 the mLN by transconjugants that had formed in the gut lumen (**Fig. 2B**). In addition, the data
243 indicated that mLN entry of the plasmid-bearing transconjugants occurred more than once in most of
244 the mice.
245 Next, we developed a mathematical model (**Supplementary information**) to explore the
246 relative contribution of reseeding (migration rate; μ) and plasmid transfer (conjugation rate per
247 mating pair; donor or transconjugant to recipient; γ) to the bacterial dynamics. We fit the model to
248 the experimental data (evenness of tags in **Fig. 2A-B**; recipient and transconjugant population sizes in
249 **Fig. S1A**; **Supplementary information**) to reveal the most likely migration and conjugation rates (**Fig.
250 2C** in red; μ = 1.78 events per day; $\gamma = 3.16\times10^{-11}$ events per CFU/g feces per day; **Supplementary**

251 **table S2**). This identified recipient reseeding as the rate limiting step in our observed plasmid transfer
252 dynamics, although the conjugation rate influenced the evenness of the plasmid tags and the time
253 until recipients were converted into transconjugants (**Fig. S5**). In our experimental system, we used
254 streptomycin to decrease colonization resistance, effectively raising the carrying capacity
255 (parametrized at 10^9 CFU/g feces for **Fig. 2C, Fig. S5**). However, since conjugation is density
256 dependent, we reasoned that the level of colonization resistance should influence our results. To test
257 the range of *Enterobacteriaceae* densities that would allow appreciable densities of transconjugants
258 (e.g. sufficient to allow invasion into new tissue reservoirs), we fixed the migration and conjugation
259 rates to the most likely values from **Fig. 2C.** We then varied the carrying capacity as a proxy for
260 colonization resistance, using the population sizes of recipients and transconjugants at the end of the
261 experiment (day 10) as a readout. While recipient densities increased proportionally to the carrying
262 capacity, the transconjugant population size remained below 10^6 CFU/g feces until the carrying
263 capacity reached 10^7 - 10^8 CFU/g feces (**Fig. 2E;** grey dotted lines). To validate this with our
264 experimental data, we re-analyzed the experimental data from **Fig. 1B-E** (pooling data from both
265 *S.*Tm^{Avir} and *E. coli* donors), correlating the donor population size at day 10 of the experiment (as a
266 proxy for colonization resistance) with the transconjugant populations in both the feces and the mLN
267 at day 10 (**Fig. S6A-B)**. As suggested by our model, transconjugant formation and reinvasion was
268 more likely in mice that harboured higher gut luminal donor densities, indicating a reduction in
269 colonization resistance (**Fig. S6A-B**). We confirmed this trend in simulations with both a higher and
270 lower conjugation rate than in our experimental system (**Fig. S6C-D**). Varying the conjugation rate
271 influenced the carrying capacity at which transconjugant population sizes reached appreciable
272 densities by the end of the simulation. This highlights a critical role for colonization resistance in
273 limiting tissue-reservoir-assisted plasmid spread dynamics, but also for the plasmid transfer rate
274 defined by the plasmid-strain association.
275
276 **Plasmids can use re-invading *S.*Tm to form a persistent tissue reservoir that survives antibiotics and**
277 **permits spread to further strains in the gut post-antibiotic treatment**
278
279 We then addressed the implications of newly formed plasmid tissue reservoirs for future
280 plasmid transfer dynamics in the gut. For this, in the first phase of the experiment, we performed the
281 same experiment as in **Fig. 1D** (using *S.*Tm 14028S Sm^R as a recipient and *E. coli* 536 P2^{cat} as a donor),
282 but on day 10 we gave mice three doses of ciprofloxacin instead of stopping the experiment (second
283 phase of the experiment; **Fig. 3A**). As before, *S.*Tm reseeded from tissue reservoirs, obtained a
284 plasmid in the gut lumen, and transconjugants carried the plasmid into host tissues (i.e. mLN) before
285 the ciprofloxacin treatment killed gut luminal populations and left only tissue-associated persisters
286 (including some of the newly formed *S.*Tm 14028S Sm^R P2^{cat} cells) to survive (**Fig. 3A, Fig. S7A**). We
287 used ampicillin in the drinking water to suppress reseeding of these tissue-associated reservoirs
288 before the third phase of the experiment. In this third phase, we introduced a secondary recipient
289 (SL1344 ΔP2) and monitored plasmid transfer (and thus the formation of secondary transconjugants)
290 to this strain. Strikingly, secondary transconjugants were formed in most mice (3/5 mice, numbered
291 1-3; **Fig. 3A, Fig. S7A**; black dots), correlating with both the presence of primary transconjugants in
292 newly formed tissue reservoirs in the mLN, and reseeding of primary transconjugants (**Fig. 3B**; **Fig.**
293 **S7B**). Importantly, *E. coli* donors were not detected in this experiment after the ciprofloxacin
294 treatment, suggesting that plasmid transfer was due to reseeding primary transconjugants from their
295 new reservoirs (**Fig. S7A-B**). A control experiment in which we euthanized a subset of mice at day 15
296 (when we normally added the secondary recipient) and investigated the tissue reservoirs verified this
297 (**Fig. S8**).
298 Next, we tested if multiple plasmids could accumulate in the gut lumen from tissue
299 reservoirs. We performed the first two phases of the experiment as above (**Fig. 3A-B**), but this time

300 in the third phase of the experiment, we added a second *E. coli* donor containing an extended-
301 spectrum beta-lactamase (ESBL) resistance plasmid (pESBL) shown to conjugate efficiently both in
302 antibiotic pre-treated mice and mice containing a reduced complexity microbiota (2, 40). As in the
303 previous experiment, $P2^{cat}$ transconjugants were formed in the first phase of the experiment,
304 followed by the elimination of bacteria from the gut lumen and storage of $P2^{cat}$ transconjugants in
305 tissue reservoirs in the second phase of the experiment (**Fig. 3C**; **Fig. S7C-D**). Following the
306 introduction of pESBL donors, pESBL transconjugants were detected in most mice (4/7 mice) as
307 additional recipients reseeded from their reservoirs (**Fig. 3C; Fig. S7C**). Importantly, in 2 of these 4
308 mice (labeled "a" and "b", $P2^{cat}$ transconjugants were also detected in the feces, suggesting that $P2^{cat}$
309 transconjugants reseeded from their reservoirs (**Fig. 3C; Fig. S7C**). As in the other experiments, pESBL
310 transconjugants could also be detected in the mLN of one mouse (**Fig. 3D**). These data indicate that
311 invasive enteropathogens like *S.*Tm might allow different resistance plasmids to accumulate in tissue
312 reservoirs in the long run. However, it is important to reiterate that invasion into the mLN is likely
313 influenced by priority effects, making each subsequent invasion less likely. This may explain why both
314 types of transconjugants were not found in the same mLN in the tested mice (mouse "a" and "b"; **Fig.**
315 **3D**). Nevertheless, the accumulation of two plasmids in the gut lumen can be facilitated by tissue
316 reservoirs.
317 Altogether, this indicates that tissue reservoirs of *S.*Tm can influence plasmid spread in the
318 gut both by spreading plasmids to different recipients over time, or accumulating multiple plasmids
319 over time.
320
321 **ESBL resistance plasmids can facilitate reseeding of *S.*Tm from tissue reservoirs under beta-lactam**
322 **treatment, and promote their spread**
323
324 Plasmids are selfish genetic elements that can use persistent pathogen cells to form long
325 term-reservoirs in host tissues. We reasoned that some plasmids (e.g. those encoding for resistances
326 that can clear antibiotics nearby, such as beta-lactamases) may have another way to promote such
327 transconjugant-dependent reservoir formation by protecting potential recipients in their
328 surroundings. The survival of *S.*Tm in the presence of otherwise lethal concentrations of beta-lactam
329 antibiotics mediated by ampicillin-resistant *E. coli* has been described *in vitro*, based on the
330 extracellular acting mechanism of beta-lactamases (26). Furthermore, antibiotic treatment (of which
331 beta-lactams comprise a large fraction) is commonly used in the treatment of bacterial infections in
332 humans and livestock (25, 41, 42). Therefore, we asked if gut luminal *Enterobacteriaceae* harbouring
333 plasmids that confer resistance to the antibiotic used could facilitate survival of *S.*Tm recipients long
334 enough to obtain a plasmid and survive in the gut lumen. As a class of multi-drug resistance plasmids
335 that has drawn particular attention as a contributor to antibiotic resistance spread, and because of
336 their extracellular mechanism of action, we chose to study ESBL plasmids under beta-lactam
337 treatment (25, 43-45).
338 As previously, we infected *S.*Tm recipients (14028S Sm^R) i.p. into mice. One day post
339 infection, we introduced *E. coli* orally either bearing pESBL (same strains used in **Fig. 3C-D**; clinical
340 isolate characterized and sequenced in (2, 40)), or $P2^{cat}$ as a control (isogenic *E coli* strains; the $P2^{cat}$ *E.*
341 *coli* was cured of pESBL, followed by *in vitro* conjugation of $P2^{cat}$), and simultaneously gave the mice
342 ampicillin in the drinking water (**Fig. 4**). Treating mice with 0.5 g/L ampicillin in the drinking water
343 corresponds to a daily dose of 2-6g in a 70 kg human, close to the recommended treatment schedule
344 of oral ampicillin of 500mg every 6 hours (46). As expected, *E. coli* pESBL grew to high densities,
345 whereas in the control animals inoculated with ampicillin susceptible *E. coli* $P2^{cat}$ (negative control
346 donors; chloramphenicol resistance), the *E. coli* could not survive (**Fig. S9A**). Over time, *S.*Tm began
347 reseeding from their tissue reservoirs in both groups of mice (**Fig. S9B**), but could only bloom in the
348 gut lumen in the presence of pESBL *E. coli* (**Fig. 4A**). This was associated with transfer of the pESBL,

349 followed by clonal expansion as *S.*Tm became resistant to ampicillin, leading to >99% of the *S.*Tm gut
350 luminal population obtaining a plasmid (**Fig. 4B**). Importantly, since *S.*Tm is an enteric pathogen that
351 utilizes inflammation to bloom in the gut (47), using an ELISA for fecal lipocalin-2, inflammation was
352 detected in mice with pESBL *E. coli*, and reached particularly high levels in mice where reseeding of
353 *S.*Tm occurred early during the experiment (i.e. >10^3 lipocalin-2 ng/g feces; **Fig. 4C**). Interestingly,
354 low-grade inflammation was detected in the absence of gut luminal *S.*Tm (**Fig. 4C**) and could suggest
355 that systemic *S.*Tm may contribute to low-grade gut inflammation, propagated by gut luminal *E. coli*.
356 To confirm that reseeding of *S.*Tm was dependent on lowering the concentration of fecal ampicillin
357 by pESBL *E. coli*, we measured the concentration of fecal ampicillin using mass spectrometry (**Fig.**
358 **4D**). In the presence of *E. coli* ESBL, fecal ampicillin concentrations plummeted below the minimum
359 inhibitory concentration (MIC; detected *in vitro* (2)) of *S.*Tm (**Fig. 4D**), likely explaining the reseeding
360 dynamics. Thus, donor mediated antibiotic degradation may protect the re-seeding recipients and
361 thereby promote pESBL transfer. Importantly, as in the previous experiments, *S.*Tm transconjugants
362 formed new plasmid reservoirs in host tissues, primarily in the mLN (**Fig. 4E**). This indicates that ESBL
363 plasmids promote their spread in host-associated *Enterobacteriaceae* in two different ways: by
364 lowering local antibiotic concentrations that ensure survival of potential recipients, and by subverting
365 tissue-lodged pathogens (persisters and growing populations alike) to form long-term reservoirs
366 within host tissues.
367
368 **Discussion:**
369
370 Our results suggest that plasmids can leverage facultative intracellular enteropathogenic
371 bacteria to promote both the formation of plasmid reservoirs in host tissues, and the spread of
372 plasmids into and among gut luminal microbes passing through a given host. In our experiments
373 using *S.*Tm infection in mice, repeated cycles of pathogen invasion and tissue reservoir formation
374 followed by reseeding the gut lumen allow plasmids to form long-term reservoirs in the host's tissues
375 (**Fig. S10, steps 1-5**). These reservoirs act as a record of gut luminal horizontal gene transfer, here
376 shown by conjugation (**Fig. 1-4**). By assessing the genetic element's tissue reservoir formation, our
377 current study significantly extends the ecological implications of our previous work where we had
378 focused on persisters, showing that these antibiotic persisters can promote the release of donors
379 into the gut lumen (2). Here we show that tissue reservoirs can influence plasmid dynamics also
380 without selection for persister survival in antibiotic treated tissues (**Fig. S10, step 1**). Most likely, it
381 will therefore happen during persistent infection involving phenotypically susceptible pathogen cells.
382 Since a natural ecological succession of *Enterobacteriaceae* has been documented in the gut (21, 24),
383 an overarching reseeding-conjugation-reinvasion cycle could result in the distribution of different
384 alleles in the various strains colonizing a host. The host tissue reservoirs would dramatically expand
385 the time scale of such transfer thereby enabling horizontal gene transfer even when the initial donor
386 and the later recipient have never "co-existed" within the host. This could pertain to resistance genes
387 or virulence determinants alike. In line with this hypothesis, different strains of commensal and
388 pathogenic Enterobacteriaceae that show vastly different plasmid, prophage and mutational profiles
389 are often observed within a given host population or even within the same host (21-23, 48, 49).
390 Conversely, the same plasmid has been detected in different enterobacterial strains over time within
391 the same patient (24). The role of the pathogen's reseeding-acquisition-reinvasion cycles in
392 resistance plasmid transfer may be particularly important in cases where different *S.*Tm are present
393 within the same host (e.g. the gut lumen vs. the host tissues), as observed in pig farms (23).
394 Which factors limit plasmid storage and transfer from host-tissue reservoirs? Through
395 population dynamic analysis, we showed that reseeding of recipient strains from tissue reservoirs is
396 the rate-limiting step for the formation of new transconjugant reservoirs (**Fig. 2; Fig. S10, step 2a**).
397 This is in line with our previous work (2) where we suggested that donor-reseeding from persister

398 reservoirs in host tissues is a rate limiting process, and reinforces the importance of understanding
399 the mechanisms of reseeding, host tissue invasion and the formation of new tissue reservoirs.
400 Previous studies have suggested the gall bladder as a route of reseeding for *Salmonella* via bile
401 secretions (16, 50, 51). In our experimental model, we found that sequence tags in the gall bladder
402 did not necessarily correlate with those found at highest density in the feces, suggesting, along with
403 others (16), that additional routes of reseeding may exist. Phagocytic cells such as macrophages and
404 dendritic cells serve as reservoirs for *S.*Tm (10-13, 20, 52) and can be reactivated by IFNγ depletion
405 (14). The high density of *S.*Tm in the tissues that line the small intestine including the gut associated
406 lymphoid tissues (here called S.I. GALT), correlating with *S.*Tm found in the gut lumen of the small
407 intestine, could suggest that trafficking of *S.*Tm-bearing immune cells to these sites (53) contributes
408 to gut luminal reseeding, but further work is needed for confirmation.

409 Interventions such as vaccination have shown success in reducing the formation of tissue
410 reservoirs and consequently plasmid transfer dynamics associated with reseeding (2, 28, 54). Here,
411 we showed that once reseeding occurred, the transfer of plasmids followed by reinvasion is likely,
412 given a sufficiently high carrying capacity (as a proxy for decreased colonization resistance) in the gut
413 lumen. This is because plasmid transfer is dependent on both the density of donors and recipients.
414 Invasion may also be density dependent (55); approximately 300 invasion events occur into the mLN
415 per day initially in streptomycin pretreated mouse models (56) and this likely decreases
416 proportionally with colonization. In a healthy microbiota community, colonization resistance
417 prohibits enterobacteriaceal blooms in >90% of the hosts (57, 58) and dramatically reduces the
418 efficiency of plasmid transfer (29, 30). However, gut perturbations such as diet shifts, inflammation,
419 antibiotic treatment, or a reduction in microbiota complexity (e.g. dysbiosis) can all lead to increases
420 in loads of *Enterobacteriaceae* and consequently plasmid transfer (**Fig. S10, step 3)** (2, 29, 30, 40, 47,
421 59, 60). Therefore, a healthy microbiota is integral in minimizing pathogen evolution in two
422 complementary ways, by reducing horizontal gene transfer and by reducing the likelihood of re-
423 invasion and subsequent formation of tissue reservoirs. Further work will be needed to validate how
424 such perturbations accelerate the dynamics of plasmid spread and reservoir formation.

425 Lastly, we showed that plasmids encoding secreted antibiotic degrading enzymes can
426 promote their own spread by an additional mechanism *in vivo*: protecting potential new recipients
427 sensitive to the antibiotic (**Fig. S10, step 2b**). Reseeding of *S.*Tm, initially susceptible to the beta-
428 lactam, can occur even in the presence of the antibiotic, dependent on the presence of *E. coli*
429 producing beta-lactamase (**Fig. 4**). The prevalence of ESBL-producing *E. coli* is rising in recent years,
430 and ESBL genes are frequently plasmid-encoded (25, 61, 62). The extracellularly acting beta-
431 lactamases are therefore public goods. *In vitro* this was shown to allow the survival of susceptible
432 *S.*Tm in the presence of otherwise lethal concentrations of ampicillin (26). In our experiments, we
433 showed that the same process occurs in the gut lumen, with reseeding *S.*Tm followed by conjugation,
434 clonal expansion, and tissue reinvasion as a consequence (**Fig. 4**). As one of the prodigal mechanisms
435 for blooms (of resistant bacteria), antibiotic treatment could serve to amplify reseeding followed by
436 plasmid exchange and tissue reservoir reformation, given sufficient protection from the antibiotic *in*
437 *trans.* This obviously depends on the presence of tissue-invasive enteropathogens in the hosts, which
438 is quite common in today's farming industry (23, 63), as well as the mechanism of action of the
439 antibiotic used. Conversely, pathogen intrinsic mechanisms transiently promoting survival may
440 further prolong recipient survival in an antibiotic loaded gut lumen and thereby further promote
441 plasmid spread. The transient overexpression of efflux pumps was shown to confer survival long
442 enough to obtain a plasmid in the presence of tetracycline above the MIC *in vitro* (64). Further work
443 will be necessary to determine if reseeding can be facilitated in the presence of antibiotics,
444 depending on the specific resistance genes (other than ESBLs) encoded on plasmids in strains
445 colonizing the gut lumen.

446 Overall, here we show that plasmids can subvert tissue-associated pathogen reservoirs to
447 promote long-term carriage within the host and subsequent spread. There seem to be two types of
448 tissue reservoirs with partially complementary features (**Fig. S10**). The tissue-associated reservoirs
449 formed by enteropathogens in chronic (persistent) infections are relatively large and facilitate re-
450 seeding of the gut lumen and subsequent plasmid transfer at relatively high rates. In contrast,
451 persistent pathogen cells are less frequent and need to re-start growth before engaging in any
452 luminal plasmid transfers, likely making them less efficient at luminal re-seeding. However, they
453 ensure survival of recipients and plasmid reservoir maintenance even in cases of therapy with
454 antibiotics to which these persisters are genetically susceptible. Although in our experimental model
455 plasmids can benefit strongly from tissue reservoirs, their actual transfer is dependent on the strain
456 densities in the gut lumen. Our study provides a proof of concept that tissue reservoirs can act as a
457 record of evolutionary events such as plasmid transfer in the gut lumen. It is conceivable that
458 mutational events or transfer of other mobile genetic elements, for example bacteriophages carrying
459 accessory genes, could also be stored in tissue reservoirs. Regardless, it remains to be seen how
460 often such cases occur in nature, since our work identifies these processes to be dependent on the
461 carrying capacity in the gut and conjugation rates of plasmid-strain pairs, and to what extent this
462 contributes to the dissemination of accessory genes on mobile genetic elements, such as antibiotic
463 resistance genes.

464 **Figure captions:**
465
466 **Figure 1. *S.*Tm in tissue reservoirs can reseed the gut lumen, obtain a plasmid from**
467 **Enterobacteriaceae in the gut lumen, and form new plasmid-bearing reservoirs. A)** Proposed
468 hypothesis. *S.*Tm recipients (green) establish tissue reservoirs after intraperitoneal injections and
469 spread to organs, dependent on the Type-three secretions system-2 (TTSS-2; encoded on SPI-2). The
470 microbiota (grey) provides colonization resistance against colonization of the gut lumen. Donors
471 (blue) colonize the gut lumen by an oral infection following a streptomycin treatment to suppress the
472 microbiota. *S.*Tm recipients reseed from their reservoirs and obtain a plasmid from donors forming a
473 transconjugant (red). These transconjugants then form new tissue reservoirs. **B)** Transconjugants are
474 formed in the gut lumen. Mice were i.p. infected with 10^3 CFU of a 1:1:1 mix of 14028S Sm^R *TAG1-3*
475 (*S.*Tm^{WT}; n=13) or 10^3 CFU of 14028S^{SPI-2} SmR (*S.*Tm^{SPI-2}; *ssaV* mutant; n=8). On day 2 post infection,
476 20 mg of streptomycin was given 4 hours before $5x10^7$ CFU of a 1:1:1:1 mix of *S.*Tm^{Avir} (*invG ssaV*
477 mutant) $P2^{TAG4-7}$. Selective plating was used to determine the fecal transconjugant loads. **C)** Tissue
478 reservoirs of *S.*Tm. Organs of mice in **panel B** were analyzed for recipients (green circles) or
479 transconjugants (red circles). **B-C)** Dotted line indicates the detection limit. A two-tailed Mann
480 Whitney-U test was used to compare *S.*Tm^{WT} (solid circles) to *S.*Tm^{SPI-2} (hollow circles) in each sample
481 ($p>0.05$ not significant (ns), $p<0.05$ (*), $p<0.01$ (**), $p<0.001$ (***), $p<0.0001$ (****)). **D)** *S.*Tm
482 recipients can obtain $P2^{cat}$ from *E. coli*. Mice were i.p. infected with 10^3 CFU of 14028S Sm^R *TAG1*
483 (*S.*Tm^{WT}; n=12). On day 2 post infection, 20 mg of streptomycin was given 4 hours before $5x10^7$ CFU
484 of *E. coli* 536 $P2^{cat}$. Selective plating and colony colour on MacConkey agar was used to determine the
485 fecal transconjugant loads. **E**) Tissue reservoirs of *S.*Tm after conjugation with *E. coli*. Organs in **panel**
486 **B** were analyzed for recipients (green squares) or transconjugants (red squares). **D-E)** Dotted line
487 indicates the detection limit. **B,D)** Bars indicate median. **C,E)** Lines indicate median. GB = gall bladder;
488 mLN = mesenteric lymph node. **B-E)** Fecal populations of donors, recipients, and transconjugants are
489 presented in **Fig. S1**.
490
491 **Figure 2. Reseeding from tissue reservoirs is a rate limiting step that suffices in conjugation and**
492 **formation of new reservoirs given a sufficient carrying capacity. A-B)** Mice in **Fig. 1** where reseeding
493 of recipients occurred (n=10) were analyzed for the distribution of sequence tags in enrichments of
494 recipients at day 10 of the experiment (including transconjugants) by qPCR (raw tag data shown in
495 **Fig. S4**). The dotted line indicates the conservative detection limit. Lines indicate the median. The
496 proportions of tags are plotted relative to all 7 tags (3 recipient and 4 plasmid tags). **A)** Recipient tags
497 and **B)** plasmid tags were sorted according the most abundant recipient or plasmid tag in the feces,
498 in each mouse. GB = gall bladder; mLN = mesenteric lymph node. **C)** Fitting of simulations to
499 experimental data. Individual summary statistics used to fit simulations are shown in **Fig. S5**.
500 Parameters and method for fitting is described in **Supplementary information.** The migration rate of
501 $\mu=1.78$ events per day and the conjugation rate of $\gamma=3.16x10^{-11}$ events per CFU/g feces per day
502 provide the best fit to the experimental data (red indicates rate pairs that fit the experimental data
503 most often). **D)** The migration and conjugation rates were fixed to the most likely values in **panel C**
504 and the carrying capacity was varied. Recipient (green) and transconjugant (red) populations at the
505 end of the simulation (day 10; n=100 simulations per carrying capacity) are shown as the mean with
506 the range of values. The lowest value was set to 1 CFU/g feces to allow visualization on a log scale.
507 The grey dotted lines correspond to the carrying capacity at which transconjugants are present at 10^6
508 CFU/g feces, as a density threshold that we speculate should facilitate some frequency of invasion
509 into tissue reservoirs.
510
511 **Figure 3. Newly formed plasmid reservoirs can spread plasmids to recipients after antibiotic**
512 **treatment and plasmids can accumulate in the gut dependent on tissue reservoirs. A)** *S.*Tm

transconjugants can conjugate to secondary recipients after survival of antibiotic treatment, by survival in tissue reservoirs. Mice were i.p. infected with 10^3 CFU of 14028S Sm^R *TAG1* (Kan^R; n=5). On day 2 post infection, 20 mg of streptomycin was given 4 hours before $5x10^7$ CFU of *E. coli* 536 $P2^{cat}$ (CmR). Selective plating and colony colour on MacConkey agar was used to determine the fecal transconjugant loads (red circles). On day 10, mice were given 3 mg ciprofloxacin for three days in a row, along with 2 g/l ampicillin in the drinking water from day 11-15. On day 15, a secondary recipient (SL1344 ΔP2; Amp^R) was added ($5x10^7$ CFU oral). Selective plating allowed the enumeration of secondary transconjugants (black circles). Bars indicate the median. Dashed black lines connect primary or secondary transconjugant populations of the same mice (mice are numbered 1-3; the same numbering is used in **panel B**). **B)** Tissue reservoirs of *S.*Tm. Organs of mice in **panel A** were analyzed for primary transconjugants and secondary transconjugants. Lines indicate the median. GB = gall bladder; mLN = mesenteric lymph node. The numbers correspond to the same mouse numbering as in **panel A**. **C)** *S.*Tm recipients can allow the formation of multiple transconjugants over time dependent on multiple reseeding events. Mice (n=7) were i.p. infected with recipients 14028S Sm^R *TAG1* (Kan^R) and donors *E. coli* 536 $P2^{cat}$ (CmR) as in **panel A**. On day 10, mice were given antibiotics as in **panel A**. On day 15, a second donor, (*E. coli* pESBL; Amp^R) was added ($5x10^7$ CFU oral). Selective plating allowed the enumeration of both $P2^{cat}$ (red squares) and pESBL transconjugants (grey sqares). Bars indicate the median. **D)** Tissue reservoirs of *S.*Tm. Organs of mice in **panel C** were analyzed for $P2^{cat}$ and pESBL transconjugants. Lines indicate the median. GB = gall bladder; mLN = mesenteric lymph node. Dashed lines connect the two transconjugant populations in the same fecal sample (two mice harbor both types of transconjugants: mouse (a) and (b); these mouse labels are also shown on the mLN population). **A-D)** Dotted lines indicate the detection limits. Population sizes of all strains and subpopulations are presented in **Fig. S7**.

Figure 4. Reseeding of *S.*Tm followed by reception of a plasmid and storage in new tissue reservoirs can occur under beta-lactam counter-selection, dependent on *E. coli* conjugative ESBL plasmids. A-E) Mice were i.p. infected with 10^3 CFU of a 1:1:1:1:1:1:1 mix of 14028S Sm^R *TAG1-7* (Kan^R). On day 1 post infection, mice were given 0.5 g/l ampicillin in the drinking water and either $5x10^7$ CFU of *E. coli* $P2^{cat}$ (Cm^R; black circles; n=10) or *E. coli* pESBL (Amp^R; orange circles; n=10). Dotted lines indicate detection limits. Lines connect medians on each day. A two-tailed Mann Whitney-U test was used to compare *S.*Tm^{WT} + *E. coli* $P2^{cat}$ to *S.*Tm^{WT} + *E. coli* $P2^{cat}$ in each sample ($p>0.05$ not significant (ns), $p<0.05$ (*), $p<0.01$ (**), $p<0.001$ (***), $p<0.0001$ (****)). **A)** Reseeding *S.*Tm was analyzed by selective plating on kanamycin-containing MacConkey agar. **B)** Conjugation was determined by selective and/or replica plating. **C)** Inflammation was quantified using an ELISA for fecal lipocalin-2. **D)** Fecal ampicillin was measured using mass spectrometry. The blue dashed line indicates the minimum inhibitory concentration of *S.*Tm *in vitro* (2). The red dashed line indicates the concentration of ampicillin given to the mice in the drinking water. **E)** Organs were analyzed for transconjugant populations on day 10 of the experiment. GB = gall bladder; mLN = mesenteric lymph node.

554 **Materials and methods:**

555

556 **Strains, plasmids, and primers used in this study**

557

558 Bacterial strains used in this study are derivatives of *S.*Tm SL1344 (65), *S.*Tm ATCC 14028S
559 (66), *E. coli* 536 (36, 67), or *E. coli* ESBL15 (2, 68), and are listed in **Table 1**. For cultivation of bacterial
560 strains, lysogeny broth (LB) medium was used containing the appropriate antibiotics (50 µg/ml
561 streptomycin (AppliChem); 50 µg/ml kanamycin (AppliChem); 15 µg/ml chloramphenicol
562 (AppliChem); 100 µg/ml ampicillin (AppliChem)) at 37°C (or 30°C if containing pCP20 or pCP20-IncI1).
563 Genetic constructs (e.g. gene deletions, neutral isogenic sequence tags, or the P3 plasmid) were
564 introduced into the desired background strain using P22 HT105/1 *int-201* phage transduction (69).
565 Bacterial plasmids used to confer resistance or for construction of strains are listed in **Table 2** and
566 were transformed into cells using electroporation.
567 *E. coli* ESBL 15 was cured of its plasmid, pESBL, using plasmid incompatibility. To create an
568 incompatible plasmid, pCP20-IncI1 was cloned using the replicon of pESBL. A PCR amplicon of the
569 replication initiation protein of pESBL with 831 and 420 bp upstream and downstream flanking
570 regions, respectively (to ensure the entire replicon was cloned), was cloned into pCP20 digested with
571 *Pst*I and *Eco*RV (removing the ampicillin resistance cassette) using Gibson Assembly (NEB; protocol as
572 described by the manufacturer). The resulting plasmid, pCP20-IncI1, was electroporated into *E. coli*
573 ESBL15 and grown at 30°C under chloramphenicol selection. Loss of resistance of ampicillin (and
574 consequently loss of pESBL) was confirmed by streaking on LB with ampicillin. The resulting clones
575 were restreaked on LB without chloramphenicol grown at 37°C to cure pCP20-IncI1.
576 Conjugative plasmids were transferred into the desired strain (e.g. $P2^{cat}$ into *E. coli* ΔpESBL
577 and *E. coli* 536) using *in vitro* conjugation assays. In brief, 10^5 CFU from an overnight culture of the
578 donor strain (SL1344 $P2^{cat}$) was mixed with the desired recipient, allowing conjugation overnight at
579 37°C on a rotating wheel. Cells were plated on selective MacConkey agar to identify transconjugants
580 by resistance phenotype and/or colour (i.e., *S.*Tm is *lac* negative and thus forms yellow colonies on
581 MacConkey agar while *E. coli* is *lac* positive and forms red colonies).
582 All strains and plasmids were genotyped prior to use using the primers listed in **Table 3**.

583

584 **Table 1. Strains used in this study**

Strain name	Strain Number	Relevant genotype	Resistance*	Reference
SL1344	SB300	Wild-type	Sm	(65)
ATCC 14028S	14028S	Wild-type	None	(66)
SL1344 $P2^{cat}$	M995	*cat* on P2	Sm, Cm	(30)
SL1344 ΔP2	M1404	P2 cured	Sm	(30)
E. coli 536	Z2366	Wild-type	Sm	(36, 67)
E. coli 536 $P2^{cat}$	Z2124	*cat* on P2	Sm, Cm	This study
SL1344 ΔP2 pM975	Z2287	P2 cured; *bla*	Sm, Amp	This study
E. coli ESBL15	Z2115	*CTX-M1 on pESBL*	Amp	(2, 68)
14028S Sm^R	T186	*strAB* on P3	Sm	This study
14028S Sm^R *TAG1*	Z2279	*WITS1-aphT*	Sm, Kan	This study
14028S Sm^R *TAG2*	Z2281	*WITS2-aphT*	Sm, Kan	This study
14028S Sm^R *TAG3*	Z2283	*WITS11-aphT*	Sm, Kan	This study
14028S Sm^R *TAG4*	T270	*WITS13-aphT*	Sm, Kan	This study
14028S Sm^R *TAG5*	T272	*WITS17-aphT*	Sm, Kan	This study
14028S Sm^R *TAG6*	T274	*WITS19-aphT*	Sm, Kan	This study
14028S Sm^R *TAG7*	T276	*WITS21-aphT*	Sm, Kan	This study
$14028S^{SPI-2}$ Sm^R	T284	*ssaV::aphT*	Sm, Kan	This study
$SL1344^{Avir}$ $P2^{TAG4}$	Z2292	*WITS13-cat* on P2; Δ*invG* Δ*ssaV*	Sm, Cm	This study

SL1344^{Avir} P2^{TAG5}	Z2293	*WITS17-cat* on P2; Δ*invG* Δ*ssaV*	Sm, Cm	This study
SL1344^{Avir} P2^{TAG6}	Z2294	*WITS19-cat* on P2; Δ*invG* Δ*ssaV*	Sm, Cm	This study
SL1344^{Avir} P2^{TAG7}	Z2295	*WITS21-cat* on P2; Δ*invG* Δ*ssaV*	Sm, Cm	This study
E. coli ΔpESBL	Z2156	pESBL cured	None	This study
E. coli ΔpESBL P2^{cat}	T305	pESBL cured; *cat* on P2	Cm	This study

585 * Relevant resistances only: Sm = ≥50 µg/ml streptomycin; Cm = ≥15 µg/ml chloramphenicol; Kan =
586 ≥50 µg/ml kanamycin; Amp = ≥100 µg/ml ampicillin.
587
588 **Table 2. Plasmids used in this study**

Plasmid name	Relevant genotype	Resistance	Reference
pM975	*bla*; used to confer ampicillin resistance	Amp	(34)
pCP20	FLP recombinase	Amp, Cm	(70)
pCP20-IncI1 (pZ2496)	FLP-*bla*::*IncI*1 replicon	Cm	This study
P3 (pRSF1010)	*strAB*	Sm	(49)
P2 (pCol1b9)	Wild-type	None	(30)
P2^{cat}	*cat*	Cm	(30)
P2^{TAG}	*WITS13, 17, 19,or 21-cat* on P2	Cm	(2)
pESBL (pESBL15)	*CTX-M-1*	Amp	(2, 68)

589
590
591 **Table 3. Primers used in this study**

Primer name	Sequence (5' to 3')	Purpose	Reference
ESBL15_repl_gibs_for	GCC AGT TAA TAG TTT GCG CAA CGT TGT TGC CAT TGC TGC ACT GAG CTA CCA TAG ATG AC	PCR amplification of *IncI*1 replicon from pEBSL for Gibson assembly	This study
ESBL15_repl_gibs_rev	TAC AAT TAT TCC TTA CTA TGG ACA AAA ACA TCA ATC TGA T GTG GTT TCA GAA CGG TGA G	PCR amplification of *IncI*1 replicon from pEBSL for Gibson assembly	This study
ESBL15_ori_ver_up	CCA GTT AAT AGT TTG CGC AAC	Validation of pCP20-IncI1 cloning	This study
ESBL15_ori_intl_ rev	CTT TCA GCG CTT TAT AGC G	Validation of pCP20-IncI1 cloning	This study
ESBL15_ori_intl_for	CTG TTC CGA TGA CCA TCT G	Validation of pCP20-IncI1 cloning	This study
ESBL15_ori_ver_dw	CTC CAG TTT AAA TAC AAG ACG	Validation of pCP20-IncI1 cloning	This study
ssaV-137F	GCAGCGTTCCAGGGTATTCC	Verification of Δ*ssaV* in the chromosome	(31)
ssaV+155R	CAGCAAGTTCTTCTCCAGGC	Verification of Δ*ssaV* in the chromosome	(31)
invG-134F	GAAGGCCACGAGAACATCAC	Verification of Δ*invG* in the chromosome	(31)
invG+112R	GCGGCCTGTTGTATTTCCGC	Verification of Δ*invG* in the chromosome	(31)
P3_SmR_for	CTA GTA TGA CGT CTG TCG C	Verification of P3	This study
P3_SmR_rev	CAC GTT TCG CAA CCT GTT C	Verification of P3	This study
WITS1	ACG ACA CCA CTC CAC ACC TA	qPCR for TAG1	(39)
WITS2	ACC CGC AAT ACC AAC AAC TC	qPCR for TAG2	(39)
WITS11	ATC CCA CAC ACT CGA TCT CA	qPCR for TAG11	(39)
WITS13	GCT AAA GAC ACC CCT CAC TCA	qPCR for TAG13	(39)
WITS17	TCA CCA GCC CAC CCC CTC A	qPCR for TAG17	(39)
WITS19	GCA CTA TCC AGC CCC ATA AC	qPCR for TAG19	(39)
WITS21	ACA ACC ACC GAT CAC TCT CC	qPCR for TAG21	(39)
ydgA	GGC TGT CCG CAA TGG GTC	qPCR for all tags	(39)

592
593 **Infection experiments**
594
595 All animal experiments were performed in 8-12 week-old specified opportunistic pathogen-
596 free (SOPF) 129/SvEv mice. These mice contain a functional *Nramp1* allele (also known as *Slc11a1*)

597 and are resistant to *S.*Tm and therefore allow for long-term infections (32, 33). All infection
598 experiments were approved by the responsible authorities (Tierversuchskommission, Kantonales
599 Veterinäramt Zürich, licenses 193/2016 and 158/2019). Sample size was not predetermined and mice
600 were randomly assigned to treatment groups.
601 For all experiments, overnight cultures of recipient *S.*Tm (14028S Sm^R derivatives) containing
602 the appropriate antibiotics were washed with sterile PBS 2x before being diluted to 10^4 CFU/ml in
603 PBS. Mixtures of the appropriate strains (in the case of tagged strains) or single strains were
604 intraperitoneally injected into mice as a 100 µl volume (~10^3 CFU per mouse). All mice used for
605 plasmid transfer experiments were housed in individual cages to ensure experimental independence.
606 For experiments that lasted longer than 10 days, mice were caged in pairs initially, but split to
607 individual cages for the final 10 days (due to ethical reasons, mice were not individually caged for
608 longer than 10 days).
609 On day 2 post infection, mice were given an oral dose of streptomycin (20 mg), as previously
610 described for the streptomycin pretreated mouse model (60). Overnight cultures of donor strains
611 (Sm^R; SL1344 or *E. coli* 536 derivatives) containing the appropriate antibiotics were subcultured for 4
612 hours 1:20 in 2 ml LB without antibiotics, and then washed in PBS. 4 hours after streptomycin
613 treatment, donors were given orally (~$5x10^7$ CFU per mouse). After 10 days, mice were either
614 euthanized or given doses of oral ciprofloxacin (3 mg per mouse; ciprofloxacin hydrochloride
615 monohydrate, Sigma-Aldrich, dissolved in 100 µl sterile dH_2O) for three consecutive days, while
616 ampicillin (2 g/L) was provided in the drinking water on days 11-15 to prevent reseeding before the
617 third strain was added. After each ciprofloxacin treatment, cages were changed to prevent
618 reinfection due to coprophagy. On day 15 of the experiment, mice were either euthanized, or given a
619 third strain (either a second recipient or a second donor; Amp^R). These mice were euthanized on day
620 22.
621 For mice used to enrich for persisters in tissue reservoirs (**Fig. S2**), ceftriaxone (1.5 mg
622 ceftriaxone disodium salt hemi(heptahydrate) dissolved in 100 µl PBS; Sigma-Aldrich) was injected
623 intraperitoneally for 3 consecutive days. Donors were added after a streptomycin treatment (as
624 above) on day 6 and again without streptomycin on day 8 to ensure robust colonization. These mice
625 were euthanized on day 15.
626 For mice used to investigate reseeding in the presence of ampicillin counterselection
627 dependent on ESBL-producing *E. coli* (**Fig. 4**), on day 1 post intraperitoneal infection of recipients, the
628 mice were given 0.5 g/L ampicillin in the drinking water and given ~$5x10^7$ CFU pESBL or $P2^{cat}$ *E. coli*
629 donors orally (in PBS, following a 4 hours subculture as described above). An ELISA for mouse
630 lipocalin-2 was performed on feces (protocol according to the manufacturer; R&D Systems kit) to
631 determine the inflammatory state of the gut.
632 In all mouse experiments, feces were collected daily into pre-weighed Eppendorf tubes and
633 homogenized in PBS using a steel ball at 25 Hz for 1 minute. Populations of donors, recipients, and
634 transconjugants were diluted and enumerated using selective MacConkey agar. Replica plating was
635 used to accurately determine the ratio of recipients or donors to transconjugants if transconjugants
636 were on the same order of magnitude as the donors or recipients. When mice were euthanized (at
637 day 2, 10, 15, or 22; specified in the figure legends), the spleen, liver, gall bladder, and mesenteric
638 lymph node, were collected and homogenized in PBS. Populations of bacteria were enumerated as
639 for the feces. For mice euthanized at day 2 post infection (**Fig. S3**), additional organs were collected.
640 For the duodenum, jejunum, ileum, cecum, and colon, first the content was collected, and then 1cm
641 of each tissue was opened longitudinally and washed briefly in PBS before homogenization. For the
642 purposes of this study, the small intestinal and large intestinal gut-associated lymphoid tissue (S.I.
643 and L.I. GALT) was collected by removing the lining of the tissues (including the fat) for each of the
644 small intestine and large intestine. For analysis of bacterial loads in the blood, 100 µl of blood was
645 aspirated from the heart immediately after euthanasia and collected in PBS with 2% BSA and 1 mM

646 EDTA. Blood samples were also homogenized. Dissection tools were disinfected in 70% EtOH in
647 between each organ to minimize the chance of cross-contamination between organs.
648
649 **Analysis of population dynamics using neutral sequence tags**
650
651 Mice were infected with an equal ratio of *S.*Tm 14028S Sm^R recipient strains (total ~10^3 CFU)
652 bearing sequence tags at a neutral locus in the chromosome (39). For analysis of reseeding and
653 plasmid transfer dynamics in **Fig. 2**, three recipient tagged strain were used (TAG1-3 Kan^R; 1:1:1
654 ratio). On day 2 post infection, an equal ratio of donor tagged strains (*S.*Tm $SL1344^{Avir}$ $P2^{TAG}$ strains;
655 TAG4-7 Cm^R; 1:1:1:1) were given at a total inoculum size of ~$5x10^7$ CFU per mouse orally. The inocula
656 were enriched in either LB+chloramphenicol (for donors) or LB+kanamycin (for recipients). At the end
657 of the experiment (i.e., on day 10 post infection), mice were euthanized and
658 recipient+transconjugant populations were enriched from 100 µl of the feces and organ
659 homogenates (in parallel to selective plating) in LB supplemented with kanamycin.
660 Enrichments were concentrated and genomic DNA was extracted using a QIAamp DNA Mini
661 Kit (Qiagen). qPCR analysis was performed according to temperature conditions as previously
662 described (39) using qPCR primers specific to the TAG and a universal second primer, *ydgA* (**Table 3**).
663 The relative proportion was calculated by dividing the DNA copy number (calculated from the C_T
664 value) of each tag detected, by the sum of all 7 tags in the sample. A dilution standard of purified
665 chromosomal DNA allowed for a correlation between DNA copy number and C_T value. For each qPCR
666 run, the detection limit was determined by the C_T value of the most-diluted DNA standard. The least
667 precise detection limit defines the conservative detection limit plotted on graphs and used for the
668 mathematical model ($8.9x10^{-5}$). Once the relative proportion was determined, recipient tags were
669 separated from plasmid tags (however, the proportion remains relative to all tags). This data is
670 presented in **Fig. S4**. Next, the tags were sorted according to the most abundant in the feces in each
671 given mouse (separately for recipient and plasmid tags). This ranking was conserved for analysis in
672 other organs to allow a correlation between the most abundant tag in the organs relative to the
673 feces. For example, if TAG2 appeared the most abundant in the feces but least abundant in the mLN,
674 it would ranked and coloured according to the most abundant tag, and it would still appear the same
675 colour in the mLN, despite it not being the most abundant tag in the mLN. This data is presented in
676 **Fig. 2A-B**.
677
678 **Measurement of fecal ampicillin**
679
680 Detection and absolute quantification of ampicillin was carried out using high-performance
681 liquid chromatography heated electrospray ionization high-resolution mass spectrometry (HPLC HESI
682 HRMS). Fecal samples were homogenized in PBS and immediately frozen after collection. Prior to
683 analysis, samples were thawed and centrifuged at high speed. The supernatants were analyzed on a
684 Dionex UltiMate 3000 HPLC coupled to a Q Exactive™ Hybrid Quadrupole-Orbitrap™ mass
685 spectrometer. Chromatographic separation was obtained on a Phenomenex Kinetex 2.6 µm XB-C18
686 150 × 4.6 mm column at 30°C. Water (A) and acetonitrile (B), each containing 0.1% formic acid, were
687 employed as mobile phases. A gradient of total 12.5 min was applied at a flowrate of 800 µL/min,
688 starting with 3% B for 2 min, 3% to 50% B in 3 min, 50% to 98% B in 5 min, 98% B for 1 min, 98% to
689 3% B in 1 min and 3% B for 0.5 min. MS-settings: spray voltage (+) 3.5 kV, capillary temperature 320
690 °C; sheath gas (57.50), auxiliary gas (16.25), sweep gas (3.25); probe heater 462.50°C; S-Lens RF (50),
691 resolution (70.000); AGC target (3e6), microscans (1), maximum IT 200 ms, scan range 250–750 *m/z.*
692 For quantification, an ampicillin standard curve was recorded using H_2O diluted concentrations of 10
693 ng/mL, 100 ng/mL, 500 ng/mL, 1 µg/mL, 10 µg/mL and 100 µg/mL from a 1 mg/mL ampicillin stock
694 solution. Samples were analyzed by retention time of ampicillin and the respective ion adduct $[M+H]^+$

= 350.1169 *m/z* with a mass tolerance of 5 ppm. 15 µL of each sample were injected and ampicillin concentrations were calculated using the Thermo Xcalibur 2.2 Quan Browser software. The concentration given in µg/ml of supernatant was normalized to the weight of feces collected and converted to µg/ml fecal content using the average density of feces (71).

Statistical analysis

Statistical tests on experimental data were performed using GraphPad Prism 8 for Windows. The test used is described in the figure caption. The mathematical model was fit to the experimental measurements using an Approximate Bayesian Computation (ABC) approach (72). For the fit, we considered three sets of summary statistics: the skew of the plasmid and chromosomal tag distributions, the total size of the transconjugant and recipient population on day 10, and the time at which the transconjugant and recipient populations first exceeded 10^6 CFU/g feces. A simulation was called "successful" if all summary statistics were within three standard deviations of the experimentally observed mean of these statistics. Migration and conjugation rates were varied on a grid, all other parameters were kept fixed (**Supplementary table S1**). All R-code needed to simulate the stochastic model, estimate the most likely parameters from the experimental data, and plot the results, is included in the Github repository https://github.com/JSHuisman/Recorder .

Acknowledgements:

We would like to thank the staff at RCHCI and EPIC animal facilities, and members of the Hardt, Sunagawa and Slack labs for helpful discussions. This work has been supported by grants from the Swiss National Science Foundation (NRP 72 407240_167121, 310030B_173338 and 310030_192567), the Gebert Rüf Foundation (GRS-060/18) and the Monique Dornonville de la Cour Foundation to WDH. MD is funded by an SNF professorship grant (PP00PP_176954) and a BRCCH multi-investigator grant, JSH is funded by NRP72 grant 407240-167121 from the Swiss National Science Foundation, and EB acknowledges a Boehringer Ingelheim Fonds PhD fellowship.

Contributions:

EB and WDH conceived the project and designed the experiments. EB, JAH, and EG carried out the mouse experiments and analyzed data. JSH designed and performed the mathematical modeling. RRR and SB supervised the mathematical modelling. AOB and JP measured fecal ampicillin using mass spectrometry. EB wrote the initial draft of the manuscript. EB, MD, and WDH reviewed and edited the manuscript to its final form. All authors read, commented on, and approved this manuscript.

Supplementary information:

Description of the mathematical model

We model the reseeding of Salmonella recipients from systemic sites into the gut, and the subsequent creation of transconjugants through plasmid transfer from donors. We follow the dynamics of Donor (D), Recipient (R), and Transconjugant (T) populations in the gut. These populations are further divided into isogenic subpopulations based on their sequence tags. The donors D_j carry a plasmid tag $j \in 1 \ldots N_j$, where N_j is the number of plasmid tags ($N_j = 4$). Recipients R_i carry a chromosomal tag $i \in 1 \ldots N_i$, where N_i is the total number of chromosomal tags ($N_i = 3$). Transconjugants T_{ij} carry both a chromosomal and a plasmid tag.

To describe the dynamics of these populations, we make several assumptions. Recipients are introduced into the gut at an overall rate μ. Here we assume this rate is constant, although it likely increases slightly during the experiment as a function of the recipient population size at systemic sites. We assume the populations of recipients and donors in the gut are well-mixed, and plasmid transfer is described by mass-action kinetics. Plasmids are thus transferred between donors and recipients at a constant per-contact rate γ_D. Once transconjugants are formed, these can also transfer their plasmid at a constant per-contact rate γ_T. All plasmids are isogenic; they transfer from donors or transconjugants at the same rate and can be transferred only to naïve recipients.

Resources are limited in the gut, so we model bacterial population growth as a logistic function of the population size. We assume the donor population is limited by a different resource than the recipient and transconjugant populations, since they are not isogenic (35). The populations thus reach separate carrying capacities, denoted by K_D and K_{RT} respectively. Otherwise, the growth dynamics are assumed population independent: the bacteria are born at a birth-rate r, are cleared at a clearance rate c (this includes both death and efflux from the gut), and similar to (2) we parametrize this with a residual birth-rate at carrying capacity $r_K = c$ (to ensure some continued population turnover even at high densities).

We simulate the population dynamics stochastically using the tau-leaping method from the R package *adaptivetau* (73). The corresponding deterministic equations (in the limit of large numbers) are:

$$\dot{D}_j = (r + r_K)D_j - D_j\left(c + \mathrm{r}\frac{\sum_j D_j}{K_D}\right) \#(1)$$

$$\dot{R}_i = (r + r_K)R_i + \frac{1}{N_i}\mu - \sum_j\left(\gamma_D D_j + \gamma_T \sum_i T_{ij}\right)R_i - R_i\left(c + \mathrm{r}\frac{\sum_i(R_i + \sum_j T_{ij})}{K_{RT}}\right) \#(2)$$

$$\dot{T}_{ij} = (r + r_K)T_{ij} + \left(\gamma_D D_j + \gamma_T \sum_i T_{ij}\right)R_i - T_{ij}\left(c + \mathrm{r}\frac{\sum_i(R_i + \sum_j T_{ij})}{K_{RT}}\right) \#(3)$$

Parametrizing the mathematical model

In the main simulations, we varied the migration rate μ and the conjugation rates $\gamma_{D/T}$ while the other parameters were kept fixed (summarized in **Table S1**). The population-independent parameters describing the bacterial growth dynamics (r, c, r_K), as well as the carrying capacities $K_{D/RT}$ and inoculum density D_0, were set to the values from (2) . There they were parametrized based on experimental data from the same mouse model system (28, 60). The number of distinguishable chromosomal and plasmid tag populations match those used in this paper. We fixed the conjugation

rates from donors and transconjugants to the same value, and the carrying capacities of donors and recipients+transconjugants were set to the same value.

Table S1. Parameter values used in the simulations

Parameter	Function	Value	Units
r	Birth-rate	44 ln(2)	Per day
c	Clearance-rate	4 ln(2)	Per day
r_K	Residual birth-rate at carrying capacity	$4\ln(2)$	Per day
$K = K_{D/RT}$	Carrying capacity	10^9	CFU/g feces
D_0	Size of the donor inoculum	10^7	CFU/g feces
N_i	Number of distinguishable chromosomal tags	3	Dimensionless
N_j	Number of distinguishable plasmid tags	4	Dimensionless
μ	Reseeding rate of recipients from systemic sites	**Uniform on the discrete grid** 10^{-6} – 10^3 in 0.25 log increments	Per day
$\gamma = \gamma_{D/T}$	The rate of conjugation from donors or transconjugants per mating pair	**Uniform on the discrete grid** 10^{-12} – 10^{-3} in 0.25 log increments	Per CFU/g feces per day

Parameter estimation in the mathematical model

We use Approximate Bayesian Computation (ABC) (72) to infer the most likely values of migration rate μ and conjugation rate γ. We varied both parameters on a grid, running 100 simulations per parameter set. For each parameter combination, we calculated summary statistics (see below) to compare the simulations to the experimental data.

i. The Evenness index E of the plasmid and chromosomal tag distributions. E is defined as 1 – g where g is the Gini index (2, 74).
ii. The size of the recipient and transconjugant populations on day 10, respectively.
iii. The time at which the recipient and transconjugant populations first exceed 10^6 CFU/g feces, respectively.

For **Fig. 2C** we calculated the likelihood of the parameter combination as the percentage of simulations that return all summary statistics within three standard deviations of the experimentally observed mean of these statistics. The experimental data used to calculate the mean of these statistics is derived from **Fig. 1B, S1A,** and **Fig. 2A-B** (n=8)**.** Due to the assumptions of our model, we excluded mice where reseeding did not occur. Therefore, the migration rate calculated here may be slightly overestimated. However, we do not expect the relative importance of reseeding or conjugation to change due to the exclusion of these mice.

Table S2. Parameter estimates

Simulation	Maximum likelihood (μ,γ) pair	μ value from the marginal posterior distribution	γ value from the marginal posterior distribution
Main text (**Fig. 2D**)	μ=1.78 (per day) γ=3.16×10^{-11} (per CFU/g feces per day)	7.1 (per day) HPD: [0.03, 31.6]	9.36×10^{-10} (per CFU/g feces per day) HPD: [1×10^{-12}, 5.6×10^{-9}]

*HPD: Highest posterior density interval

Dependence of transconjugant emergence on the carrying capacity in the gut

In a separate analysis, we estimated the evenness of the plasmid and chromosomal tag distributions, as well as the final recipient and transconjugant population sizes, as a function of the carrying capacity. Here we fixed the migration rate μ and conjugation rate γ at their most likely values (μ = 1.78 per day, $\gamma = 3.16\times10^{-11}$ per CFU/g feces per day), and varied the carrying capacity K uniformly on the grid $10^3 - 10^{10}$ in 0.25 log increments.

In addition, we repeated this set of simulations with a conjugation rate that was either 100-fold higher, or 100-fold lower than the most likely value.

806 **Supplementary figure captions**
807
808 **Figure S1. Fecal populations for mice in Figure 1.** Donors (blue; Cm^R), recipients (green; Kan^R), and
809 transconjugants (red; Cm^R and Kan^R) were enumerated by selective and/or replica plating on
810 MacConkey agar. The black dotted lines represent the detection limits for transconjugants and
811 donors (and recipients in **panel B**). The green dotted lines represent the detection limits for
812 recipients. The detection limit is higher for recipients once the density of bacteria reaches $>10^8$ CFU/g
813 feces (because of the limit of colonies on a plate for replica plating). Before this happens, recipient
814 populations can appear below this line (then the black dotted line is the detection limit). Lines of
815 colour connect medians between days. **A-B)** Mice from **Fig. 1B-C** infected with $SL1344^{Avir}$ $P2^{cat}$ as
816 donors. **A)** Mice infected with *S.*Tm^{WT} recipients (n=13). **B)** Mice infected with *S.*Tm^{SPI-2} recipients
817 (n=8). **C)** Mice from **Fig. 1D-E** infected with *S.*Tm^{WT} recipients and *E. coli* 536 $P2^{cat}$ as donors (n=12).
818
819 **Figure S2. Control for reseeding and obtaining a plasmid from persisters induced by antibiotic**
820 **treatment.** Mice were i.p. infected with 10^3 CFU of 14028S Sm^R *TAG1* (Kan^R; n=7). On day 2 post
821 infection, doses of ceftriaxone (1.5 mg i.p. per mouse per day) were given for three consecutive days.
822 On day 6, 20 mg of streptomycin was given 4 hours before $5x10^7$ CFU of *E. coli* 536 $P2^{cat}$ (Cm^R). *E. coli*
823 was given again on day 8 post infection to ensure colonization. **A)** Donors (blue; Cm^R), recipients
824 (green; Kan^R), and transconjugants (red; Cm^R and Kan^R) were enumerated by selective and/or replica
825 plating on MacConkey agar. The black dotted lines represent the detection limits for transconjugants
826 and donors. The green dotted lines represent the detection limits for recipients. The detection limit is
827 higher for recipients once the density of bacteria reaches $>10^8$ CFU/g feces (because of the limit of
828 colonies on a plate for replica plating). Before this happens, recipient populations can appear below
829 this line (then the black dotted line is the detection limit). Lines of colour connect medians between
830 days. **B)** Organs of mice in **panel A** were analyzed for population sizes of recipients and
831 transconjugants. Lines indicate medians. Dotted line indicates the detection limit. GB = gall bladder;
832 mLN = mesenteric lymph node.
833
834 **Figure S3. Localization of tissue reservoirs of *S.*Tm prior to reseeding.** Mice (n=7) were i.p. infected
835 with 10^3 CFU of a 1:1:1:1:1:1:1 mix of 14028S Sm^R *TAG1-7*. At day 2 post infection, *S.*Tm in the
836 organs were enumerated. For feces and the intestinal content, pre-weighed tubes were used to
837 determine *S.*Tm per g of content. Blood is reported per ml. Intestinal tissues are reported per cm.
838 The small intestinal (S.I.) and large intestinal (L.I.) gut-associated lymphoid tissues (GALT) contain the
839 lining of the intestinal tissues, which includes the GALT (but also fat). Here, we called them S.I. and
840 L.I. GALT, but they can contain more than just this region. Dotted lines indicate the detection limits.
841 Lines indicate medians.
842
843 **Figure S4**. **Raw tag proportions before sorting and re-colouring for mice in Figure 2.** Relative tag
844 proportions detected by qPCR in the inocula (R. ino. = recipient inoculum; D. ino. = donor inoculum),
845 the feces, and the organs at day 10 of the experiment. All samples are derived from an enrichment
846 in LB+kanamycin (to enrich for recipients+transconjugants). Each tag is given a unique colour. Mice
847 are separated by vertical dashed lines. Sample groups are separated by vertical solid lines. Dotted
848 line indicates the conservative detection limit. GB = gall bladder; mLN = mesenteric lymph node. **A)**
849 Recipient tags. **B)** Plasmid tags.
850
851 **Figure S5. Summary statistics used for fitting the mathematical model to the experimental data in**
852 **Fig. 2C. A-F)** The mathematical model was fit to the experimental data using 6 metrics (described in
853 the **Supplementary information**). The values of all 6 metrics were calculated on the grid of possible
854 migration and conjugation rate pairs. For each metric, the experimentally determined mean is shown

855 in red (an arrow and red text indicates the mean value), and values of simulations that are above the
856 experimental mean are indicated in a gradient towards white, whereas values that are below the
857 experimental mean are indicated in a gradient towards black. Grey fill indicates migration and
858 conjugation rate pairs where the given metric cannot be calculated (e.g. evenness of tags cannot be
859 calculated if reseeding of recipients into the feces does not occur; the recipient population never
860 reaches appreciable densities if the conjugation rate is too high). **A)** Evenness of chromosomal tags
861 in the recipient+transconjugant fecal population at day 10 (experimental mean = 0.0166; SD =
862 0.0508). **B)** Evenness of plasmid tags in the transconjugant fecal population at day 10 (experimental
863 mean = 0.358; SD = 0.282). **C)** Days of the experiment (timeline as in **Fig. 1**) until the recipient
864 population exceeds 10^6 CFU / g feces (experimental mean = 4.875; SD = 1.642). **D)** Days of the
865 experiment (timeline as in **Fig. 1**) until the transconjugant population exceeds 10^6 CFU / g feces
866 (experimental mean = 5.00; SD = 0.926). **E)** Recipient population in the feces at day 10 (experimental
867 mean = 2.9×10^8 CFU / g feces; SD = 3.75×10^8 CFU / g feces). **F)** Transconjugant population in the feces
868 at day 10 (experimental mean = 2.61×10^8 CFU / g feces; SD = 3.45×10^8 CFU / g feces).
869
870 **Figure S6. Dependence of recipient and transconjugant population sizes on the carrying capacity**
871 **with a higher or lower conjugation rate compared to Fig. 2D, and correlation with experimental**
872 **data in Fig. 1. A-B)** Transconjugant invasion increases proportional to the carrying capacity, as a
873 proxy for colonization resistance provided by the microbiota. Correlation of the donor population
874 size at day 10 (as a measure for carrying capacity; either SL1344 *S.*Tm^{Avir} or *E. coli* 536; data from **Fig.**
875 **S1A, C;** n=25) to the transconjugant population in the feces **(panel A;** data from **Fig. S1A, C**) or
876 mesenteric lymph node (mLN; **panel B**; data from **Fig. 1C, E**). Dotted lines indicate the detection
877 limits by selective plating. A line of best fit is shown and a linear regression is performed: **A)** R^2 =
878 0.5604; F test determined non-zero slope ($p<0.0001$); **B)** R^2 = 0.4913; F test determined non-zero
879 slope ($p<0.0001$). **C-D**) Simulation data. The migration rate was fixed to the most likely values in **Fig.**
880 **2C**, but the conjugation rate was fixed to 3.16×10^{-9}, 100-fold higher than in **Fig. 2D** to test the case of
881 a plasmid with a higher conjugation rate **(panel C),** or fixed to 3.16×10^{-13}, 100-fold lower than in **Fig.**
882 **2D** to test the case of a plasmid with a lower conjugation rate **(panel D)**. The carrying capacity was
883 varied. Recipient (green) and transconjugant (red) populations at the end of the simulation (day 10;
884 n=100 simulations per carrying capacity) are shown as the mean with the range of values. The lowest
885 value was set to 1 CFU/g feces to allow visualization on a log scale. The grey dotted lines correspond
886 to the carrying capacity at which transconjugants are present at 10^6 CFU/g feces, as a density
887 threshold that we speculate should facilitate some frequency of invasion into tissue reservoirs.
888
889 **Figure S7. Additional fecal and organ populations for mice in Figure 3. A-B)** Secondary conjugation
890 experiment (circles); mice in **Fig. 3A-B**. Donors (blue; Cm^R), primary recipients (green; Kan^R), primary
891 transconjugants (red; Cm^R and Kan^R), secondary recipients (beige; Amp^R), and secondary
892 transconjugants (black; Amp^R and Cm^R) were enumerated by selective and/or replica plating on
893 MacConkey agar. **B)** Organs of mice in **panel A** were analyzed for population sizes of donors,
894 recipients and transconjugants. **C-D)** Multiple plasmids experiment (squares); mice in **Fig. 3C-D**. P2^{cat}
895 donors (blue; Cm^R), recipients (green; Kan^R), P2^{cat} transconjugants (red; Cm^R and Kan^R), pESBL donors
896 (purple; Amp^R), and pESBL transconjugants (grey; Amp^R and Kan^R) were enumerated by selective
897 and/or replica plating on MacConkey agar. **D)** Organs of mice in **panel A** were analyzed for
898 population sizes of donors, recipients and transconjugants. **A,C)** The black dotted lines represent the
899 detection limits for transconjugants and donors. The green dotted lines represent the detection
900 limits for recipients. The detection limit is higher for recipients once the density of bacteria reaches
901 $>10^8$ CFU/g feces (because of the limit of colonies on a plate for replica plating). Before this happens,
902 recipient populations can appear below this line (then the black dotted line is the detection limit).

903 Lines of colour connect medians between days. **B,D)** Lines indicate medians. Dotted line indicates the
904 detection limit. GB = gall bladder; mLN = mesenteric lymph node.
905
906 **Figure S8. Control that *E. coli* donors are not detected in tissue reservoirs after antibiotic**
907 **treatment.** Mice (n=5) were i.p. infected with 10^3 CFU of 14028S Sm^R *TAG1* recipients (Kan^R) and
908 $5x10^7$ CFU of *E. coli* 536 $P2^{cat}$ donors (CmR) as in **Fig. 3**. Selective plating and colony colour on
909 MacConkey agar was used to determine population sizes of donors (blue), recipients (green), and
910 transconjugants (red; Cm^R and Kan^R). On day 10, mice were given 3 mg ciprofloxacin for three days in
911 a row, along with 2 g/l ampicillin in the drinking water from day 11-15. **A)** Fecal population sizes. The
912 black dotted lines represent the detection limits for transconjugants and donors. The green dotted
913 lines represent the detection limits for recipients. The detection limit is higher for recipients once the
914 density of bacteria reaches >10^8 CFU/g feces (because of the limit of colonies on a plate for replica
915 plating). Before this happens, recipient populations can appear below this line (then the black dotted
916 line is the detection limit). Lines of colour connect medians between days. **B)** Organs of mice in **panel**
917 **A** were analyzed for population sizes of donors, recipients and transconjugants. Lines indicate
918 medians. Dotted line indicates the detection limit. GB = gall bladder; mLN = mesenteric lymph node.
919
920 **Figure S9. *E. coli* population sizes and total *S.*Tm population sizes in tissue reservoirs of mice in Fig.**
921 **4. A)** *E. coli* $P2^{cat}$ (Cm^R) and *E. coli* pESBL (Amp^R) populations were enumerated by selective plating
922 and colour on MacConkey agar. Coloured lined connect medians. **B)** Total *S.*Tm populations (Kan^R) in
923 organs were determined by selective plating on kanamycin MacConkey agar. GB = gall bladder; mLN
924 = mesenteric lymph node. Lines indicate the media. **A-B)** A two-tailed Mann Whitney-U test was used
925 to compare $S.Tm^{WT}$ + *E. coli* $P2^{cat}$ (black; n=10) to $S.Tm^{WT}$ + *E. coli* $P2^{cat}$ (orange; n=10) in each sample
926 ($p>0.05$ not significant (ns), $p<0.05$ (*), $p<0.0001$ (****)). Dotted lines indicate the detection limits.
927
928 **Figure S10. Working model for how the infection cycle of *S.*Tm may promote the spread and**
929 **accumulation of plasmids within a host.** Invasive *S.*Tm (green for recipients, red for transconjugants)
930 can establish reservoirs within host tissues, storing their current plasmid complement in these
931 reservoirs (n plasmids). A sub-population of these cells can survive antibiotic treatment as persisters
932 (smaller green or red cells), that can regrow after the withdrawal of antibiotics. In extension to
933 previous work (2), here we show that reservoirs of *S.*Tm that chronically infect the host can reseed
934 from host tissues, even in the absence of selection for persisters (**step 1**). Exiting the host tissues into
935 the gut lumen is a rate-limiting process (**step 2a**; (2)). This process can be facilitated by
936 Enterobacteriaceae donors (blue; plasmid shown in black) that produce extracellularly acting
937 plasmid-encoded antibiotic resistance genes (such as beta-lactamases; blue colour radiating from the
938 cell indicates local degradation of beta-lactam antibiotics by beta-lactamases), that can allow the
939 local survival of reseeding recipients under antibiotic treatment (**step 2b**). Once both donors and
940 recipients co-occur in the gut lumen at sufficient density, plasmid transfer proceeds (**step 3**; (2, 27-
941 30, 40)). When colonization resistance is relaxed, invasive transconjugants (red) can reach sufficient
942 densities to invade back into host tissues and form new reservoirs that now contain n+1 plasmids
943 (**step 4**). In the tissue, transconjugant subpopulations can also survive antibiotic therapy as persisters
944 (smaller red cells). This process is repeatable in certain conditions. Either transconjugants can reseed
945 to donate the plasmid to further gut luminal recipients (**step 5a**), or recipients can reseed to receive
946 an additional plasmids (**step 5b**). Novel steps of this process, demonstrated here using the
947 streptomycin treatment mouse model, are indicated with bold numbers, whereas steps that have
948 been previously shown are indicated with non-bold numbers (and key references are listed in the
949 caption).
950

951 **References:**
952

953 1. G. D. Wright, The antibiotic resistome: the nexus of chemical and genetic diversity. *Nat Rev*
954 *Microbiol* **5**, 175-186 (2007).
955 2. E. Bakkeren *et al.*, Salmonella persisters promote the spread of antibiotic resistance plasmids
956 in the gut. *Nature* **573**, 276-280 (2019).
957 3. N. Q. Balaban *et al.*, Definitions and guidelines for research on antibiotic persistence. *Nat Rev*
958 *Microbiol* 10.1038/s41579-019-0196-3 (2019).
959 4. B. Gollan, G. Grabe, C. Michaux, S. Helaine, Bacterial Persisters and Infection: Past, Present,
960 and Progressing. *Annu Rev Microbiol* **73**, 359-385 (2019).
961 5. I. Levin-Reisman *et al.*, Antibiotic tolerance facilitates the evolution of resistance. *Science*
962 **355**, 826-830 (2017).
963 6. J. Liu, O. Gefen, I. Ronin, M. Bar-Meir, N. Q. Balaban, Effect of tolerance on the evolution of
964 antibiotic resistance under drug combinations. *Science* **367**, 200-204 (2020).
965 7. E. M. Windels *et al.*, Bacterial persistence promotes the evolution of antibiotic resistance by
966 increasing survival and mutation rates. *ISME J* **13**, 1239-1251 (2019).
967 8. E. Bakkeren, M. Diard, W. D. Hardt, Evolutionary causes and consequences of bacterial
968 antibiotic persistence. *Nat Rev Microbiol* 10.1038/s41579-020-0378-z (2020).
969 9. M. Diard *et al.*, Antibiotic treatment selects for cooperative virulence of Salmonella
970 typhimurium. *Curr Biol* **24**, 2000-2005 (2014).
971 10. S. Helaine *et al.*, Internalization of Salmonella by macrophages induces formation of
972 nonreplicating persisters. *Science* **343**, 204-208 (2014).
973 11. D. A. C. Stapels *et al.*, Salmonella persisters undermine host immune defenses during
974 antibiotic treatment. *Science* **362**, 1156-1160 (2018).
975 12. P. Kaiser *et al.*, Cecum lymph node dendritic cells harbor slow-growing bacteria
976 phenotypically tolerant to antibiotic treatment. *PLoS Biol* **12**, e1001793 (2014).
977 13. B. Claudi *et al.*, Phenotypic variation of Salmonella in host tissues delays eradication by
978 antimicrobial chemotherapy. *Cell* **158**, 722-733 (2014).
979 14. D. M. Monack, D. M. Bouley, S. Falkow, Salmonella typhimurium persists within macrophages
980 in the mesenteric lymph nodes of chronically infected Nramp1+/+ mice and can be
981 reactivated by IFNgamma neutralization. *J Exp Med* **199**, 231-241 (2004).
982 15. T. D. Lawley *et al.*, Host transmission of Salmonella enterica serovar Typhimurium is
983 controlled by virulence factors and indigenous intestinal microbiota. *Infect Immun* **76**, 403-
984 416 (2008).
985 16. L. H. Lam, D. M. Monack, Intraspecies competition for niches in the distal gut dictate
986 transmission during persistent Salmonella infection. *PLoS Pathog* **10**, e1004527 (2014).
987 17. S. S. Grant, D. T. Hung, Persistent bacterial infections, antibiotic tolerance, and the oxidative
988 stress response. *Virulence* **4**, 273-283 (2013).
989 18. K. Endt *et al.*, Peroral ciprofloxacin therapy impairs the generation of a protective immune
990 response in a mouse model for Salmonella enterica serovar Typhimurium diarrhea, while
991 parenteral ceftriaxone therapy does not. *Antimicrob Agents Chemother* **56**, 2295-2304
992 (2012).
993 19. I. A. Onwuezobe, P. O. Oshun, C. C. Odigwe, Antimicrobials for treating symptomatic non-
994 typhoidal Salmonella infection. *Cochrane Database Syst Rev* **11**, CD001167 (2012).
995 20. T. H. M. Pham *et al.*, Salmonella-Driven Polarization of Granuloma Macrophages Antagonizes
996 TNF-Mediated Pathogen Restriction during Persistent Infection. *Cell Host Microbe* **27**, 54-67
997 e55 (2020).
998 21. J. N. V. Martinson *et al.*, Rethinking gut microbiome residency and the Enterobacteriaceae in
999 healthy human adults. *ISME J* **13**, 2306-2318 (2019).
1000 22. O. Tenaillon, D. Skurnik, B. Picard, E. Denamur, The population genetics of commensal
1001 Escherichia coli. *Nat Rev Microbiol* **8**, 207-217 (2010).
1002 23. B. San Roman *et al.*, Relationship between Salmonella infection, shedding and serology in
1003 fattening pigs in low-moderate prevalence areas. *Zoonoses Public Health* **65**, 481-489 (2018).

1004 24. R. Leon-Sampedro *et al.*, Pervasive transmission of a carbapenem resistance plasmid in the
1005 gut microbiota of hospitalized patients. *Nat Microbiol* 10.1038/s41564-021-00879-y (2021).
1006 25. WHO (2017) Global priority list of antibiotic-resistant bacteria to guide research, discovery,
1007 and development of new antibiotics. (WHO (World Health Organization)).
1008 26. M. H. Perlin *et al.*, Protection of Salmonella by ampicillin-resistant Escherichia coli in the
1009 presence of otherwise lethal drug concentrations. *Proc Biol Sci* **276**, 3759-3768 (2009).
1010 27. M. Diard *et al.*, Inflammation boosts bacteriophage transfer between Salmonella spp. *Science*
1011 **355**, 1211-1215 (2017).
1012 28. K. Moor *et al.*, High-avidity IgA protects the intestine by enchaining growing bacteria. *Nature*
1013 10.1038/nature22058 (2017).
1014 29. S. Y. Wotzka *et al.*, Escherichia coli limits Salmonella Typhimurium infections after diet shifts
1015 and fat-mediated microbiota perturbation in mice. *Nat Microbiol* 10.1038/s41564-019-0568-
1016 5 (2019).
1017 30. B. Stecher *et al.*, Gut inflammation can boost horizontal gene transfer between pathogenic
1018 and commensal Enterobacteriaceae. *Proc Natl Acad Sci U S A* **109**, 1269-1274 (2012).
1019 31. E. Bakkeren *et al.*, Cooperative virulence can emerge via horizontal gene transfer but is
1020 stabilized by transmission. *bioRxiv* 10.1101/2021.02.11.430745, 2021.2002.2011.430745
1021 (2021).
1022 32. O. Cunrath, D. Bumann, Host resistance factor SLC11A1 restricts Salmonella growth through
1023 magnesium deprivation. *Science* **366**, 995-999 (2019).
1024 33. B. Stecher *et al.*, Chronic Salmonella enterica serovar Typhimurium-induced colitis and
1025 cholangitis in streptomycin-pretreated Nramp1+/+ mice. *Infect Immun* **74**, 5047-5057 (2006).
1026 34. S. Hapfelmeier *et al.*, The Salmonella pathogenicity island (SPI)-2 and SPI-1 type III secretion
1027 systems allow Salmonella serovar typhimurium to trigger colitis via MyD88-dependent and
1028 MyD88-independent mechanisms. *J Immunol* **174**, 1675-1685 (2005).
1029 35. S. M. Lee *et al.*, Bacterial colonization factors control specificity and stability of the gut
1030 microbiota. *Nature* **501**, 426-429 (2013).
1031 36. E. Brzuszkiewicz *et al.*, How to become a uropathogen: comparative genomic analysis of
1032 extraintestinal pathogenic Escherichia coli strains. *Proc Natl Acad Sci U S A* **103**, 12879-12884
1033 (2006).
1034 37. M. Ghalayini *et al.*, Long-term evolution of the natural isolate of Escherichia coli 536 in the
1035 mouse gut colonized after maternal transmission reveals convergence in the constitutive
1036 expression of the lactose operon. *Mol Ecol* **28**, 4470-4485 (2019).
1037 38. M. Hensel *et al.*, Simultaneous identification of bacterial virulence genes by negative
1038 selection. *Science* **269**, 400-403 (1995).
1039 39. A. J. Grant *et al.*, Modelling within-host spatiotemporal dynamics of invasive bacterial
1040 disease. *PLoS Biol* **6**, e74 (2008).
1041 40. F. Benz *et al.*, Plasmid- and strain-specific factors drive variation in ESBL-plasmid spread in
1042 vitro and in vivo. *ISME J* 10.1038/s41396-020-00819-4 (2020).
1043 41. WHO, *Antimicrobial resistance: global report on surveillance* (World Health Organization
1044 (WHO), 2014).
1045 42. M. Cully, Public health: The politics of antibiotics. *Nature* **509**, S16-17 (2014).
1046 43. J. Davies, D. Davies, Origins and evolution of antibiotic resistance. *Microbiol Mol Biol Rev* **74**,
1047 417-433 (2010).
1048 44. A. Carattoli, Resistance plasmid families in Enterobacteriaceae. *Antimicrob Agents*
1049 *Chemother* **53**, 2227-2238 (2009).
1050 45. P. Bajaj, N. S. Singh, J. S. Virdi, Escherichia coli beta-Lactamases: What Really Matters. *Front*
1051 *Microbiol* **7**, 417 (2016).
1052 46. M. J. Wirfs, *The APRN and PA's Complete Guide to Prescribing Drug Therapy 2020* (Springer
1053 Publishing Company, 2019).
1054 47. B. Stecher *et al.*, Salmonella enterica serovar typhimurium exploits inflammation to compete
1055 with the intestinal microbiota. *PLoS Biol* **5**, 2177-2189 (2007).
1056 48. P. T. Desai *et al.*, Evolutionary Genomics of Salmonella enterica Subspecies. *MBio* **4** (2013).

1057 49. C. Kroger *et al.*, The transcriptional landscape and small RNAs of Salmonella enterica serovar
1058 Typhimurium. *Proc Natl Acad Sci U S A* **109**, E1277-1286 (2012).
1059 50. G. Gonzalez-Escobedo, J. M. Marshall, J. S. Gunn, Chronic and acute infection of the gall
1060 bladder by Salmonella Typhi: understanding the carrier state. *Nat Rev Microbiol* **9**, 9-14
1061 (2011).
1062 51. P. Everest, J. Wain, M. Roberts, G. Rook, G. Dougan, The molecular mechanisms of severe
1063 typhoid fever. *Trends Microbiol* **9**, 316-320 (2001).
1064 52. G. Rosenberg *et al.*, Host succinate is an activation signal for Salmonella virulence during
1065 intracellular infection. *Science* **371**, 400-405 (2021).
1066 53. A. Habtezion, L. P. Nguyen, H. Hadeiba, E. C. Butcher, Leukocyte Trafficking to the Small
1067 Intestine and Colon. *Gastroenterology* **150**, 340-354 (2016).
1068 54. K. Moor *et al.*, Peracetic Acid Treatment Generates Potent Inactivated Oral Vaccines from a
1069 Broad Range of Culturable Bacterial Species. *Front Immunol* **7**, 34 (2016).
1070 55. M. Ackermann *et al.*, Self-destructive cooperation mediated by phenotypic noise. *Nature*
1071 **454**, 987-990 (2008).
1072 56. P. Kaiser, E. Slack, A. J. Grant, W. D. Hardt, R. R. Regoes, Lymph node colonization dynamics
1073 after oral Salmonella Typhimurium infection in mice. *PLoS Pathog* **9**, e1003532 (2013).
1074 57. B. Stecher *et al.*, Like will to like: abundances of closely related species can predict
1075 susceptibility to intestinal colonization by pathogenic and commensal bacteria. *PLoS Pathog*
1076 **6**, e1000711 (2010).
1077 58. B. Stecher, W. D. Hardt, Mechanisms controlling pathogen colonization of the gut. *Curr Opin*
1078 *Microbiol* **14**, 82-91 (2011).
1079 59. M. Kreuzer, W.-D. Hardt, How Food Affects Colonization Resistance Against
1080 Enteropathogenic Bacteria. *Annual Review of Microbiology* **74** (2020).
1081 60. M. Barthel *et al.*, Pretreatment of mice with streptomycin provides a *Salmonella* enterica
1082 serovar Typhimurium colitis model that allows analysis of both pathogen and host. *Infect*
1083 *Immun* **71**, 2839-2858 (2003).
1084 61. E. Temkin, A. Adler, A. Lerner, Y. Carmeli, Carbapenem-resistant Enterobacteriaceae: biology,
1085 epidemiology, and management. *Ann N Y Acad Sci* **1323**, 22-42 (2014).
1086 62. D. Yang, Y. Guo, Z. Zhang, Combined porin loss and extended spectrum beta-lactamase
1087 production is associated with an increasing imipenem minimal inhibitory concentration in
1088 clinical Klebsiella pneumoniae strains. *Curr Microbiol* **58**, 366-370 (2009).
1089 63. T. P. Van Boeckel *et al.*, Global trends in antimicrobial resistance in animals in low- and
1090 middle-income countries. *Science* **365** (2019).
1091 64. S. Nolivos *et al.*, Role of AcrAB-TolC multidrug efflux pump in drug-resistance acquisition by
1092 plasmid transfer. *Science* **364**, 778-782 (2019).
1093 65. S. K. Hoiseth, B. A. Stocker, Aromatic-dependent *Salmonella* typhimurium are non-virulent
1094 and effective as live vaccines. *Nature* **291**, 238-239 (1981).
1095 66. T. Jarvik, C. Smillie, E. A. Groisman, H. Ochman, Short-term signatures of evolutionary change
1096 in the Salmonella enterica serovar typhimurium 14028 genome. *J Bacteriol* **192**, 560-567
1097 (2010).
1098 67. H. Berger, J. Hacker, A. Juarez, C. Hughes, W. Goebel, Cloning of the chromosomal
1099 determinants encoding hemolysin production and mannose-resistant hemagglutination in
1100 Escherichia coli. *J Bacteriol* **152**, 1241-1247 (1982).
1101 68. S. Tschudin-Sutter *et al.*, Prospective Validation of Cessation of Contact Precautions for
1102 Extended-Spectrum beta-Lactamase-Producing Escherichia coli(1). *Emerg Infect Dis* **22**, 1094-
1103 1097 (2016).
1104 69. N. L. Sternberg, R. Maurer, Bacteriophage-mediated generalized transduction in Escherichia
1105 coli and Salmonella typhimurium. *Methods Enzymol* **204**, 18-43 (1991).
1106 70. K. A. Datsenko, B. L. Wanner, One-step inactivation of chromosomal genes in Escherichia coli
1107 K-12 using PCR products. *Proc Natl Acad Sci U S A* **97**, 6640-6645 (2000).
1108 71. D. M. Brown, D. Butler, N. R. Orman, J. W. Davies, Gross solids transport in small diameter
1109 sewers. *Water Science and Technology* **33**, 25-30 (1996).

1110 72. P. Marjoram, J. Molitor, V. Plagnol, S. Tavare, Markov chain Monte Carlo without likelihoods.
1111 *Proc Natl Acad Sci U S A* **100**, 15324-15328 (2003).
1112 73. P. Johnson (2016) adaptivetau: Tau-Leaping Stochastic Simulation. (R package version 2.2.1).
1113 74. L. Maier *et al.*, Granulocytes impose a tight bottleneck upon the gut luminal pathogen
1114 population during Salmonella typhimurium colitis. *PLoS Pathog* **10**, e1004557 (2014).

1115

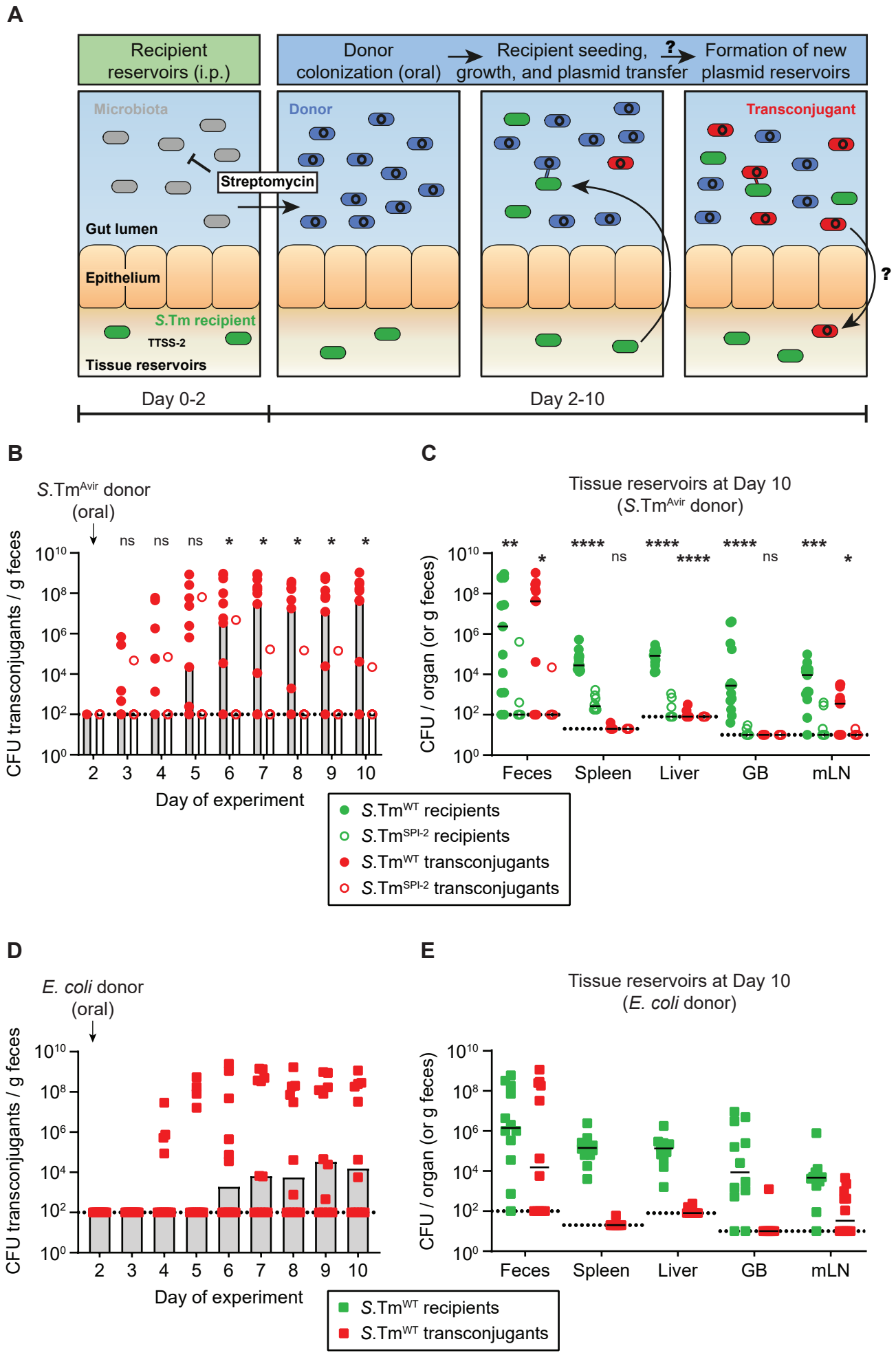

Bakkeren et al. Figure 1

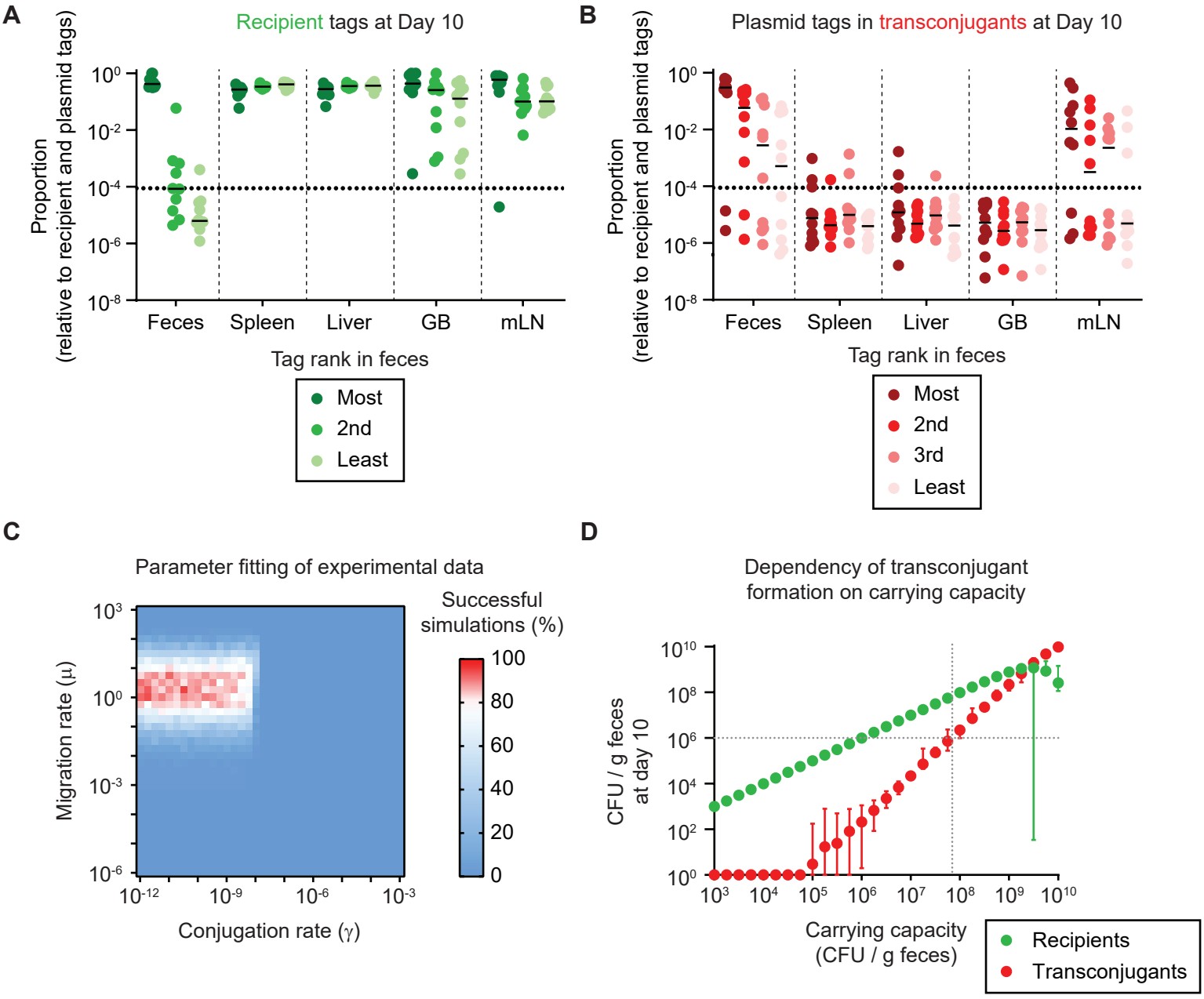

Bakkeren et al. Figure 2

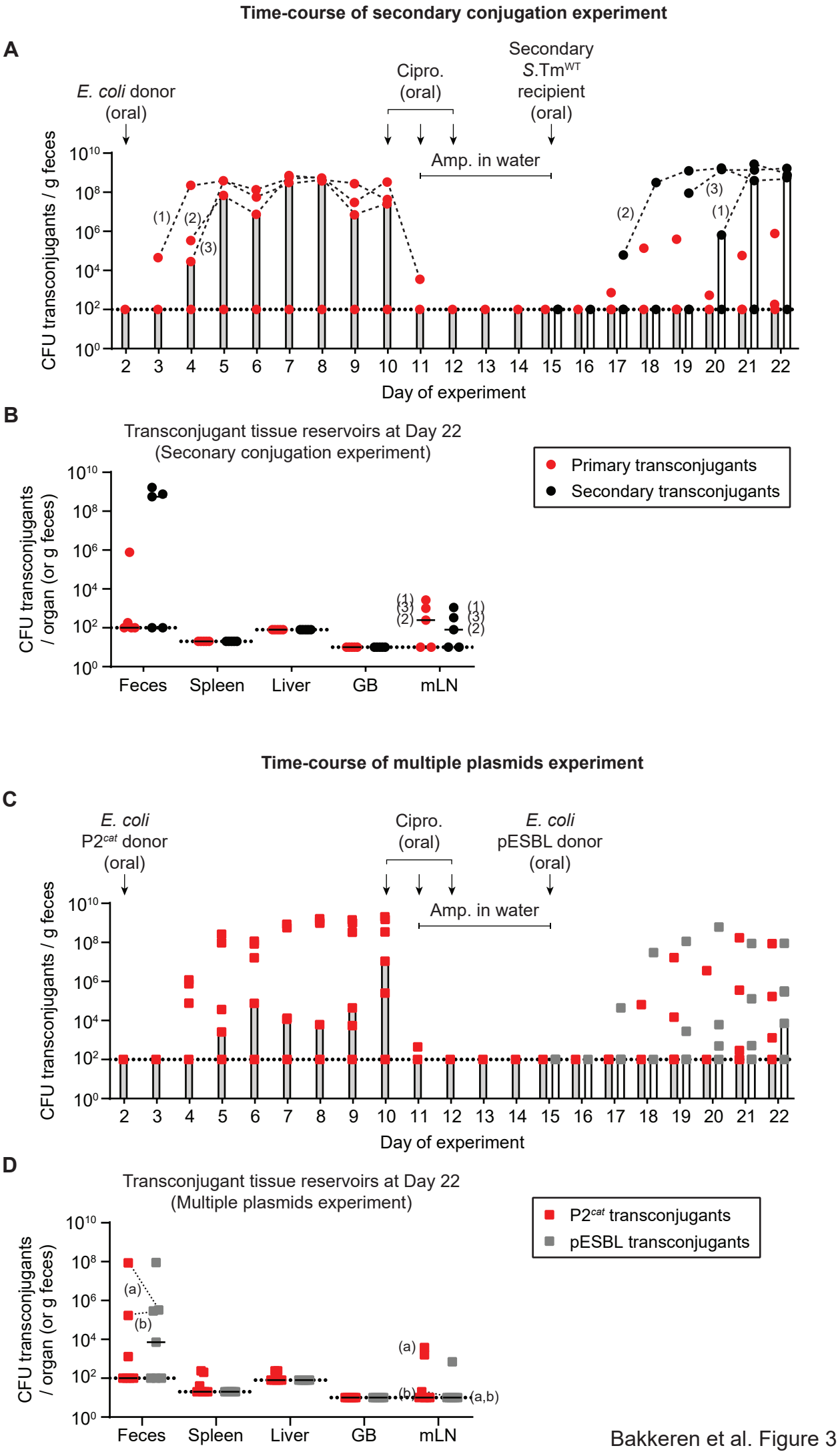

Bakkeren et al. Figure 3

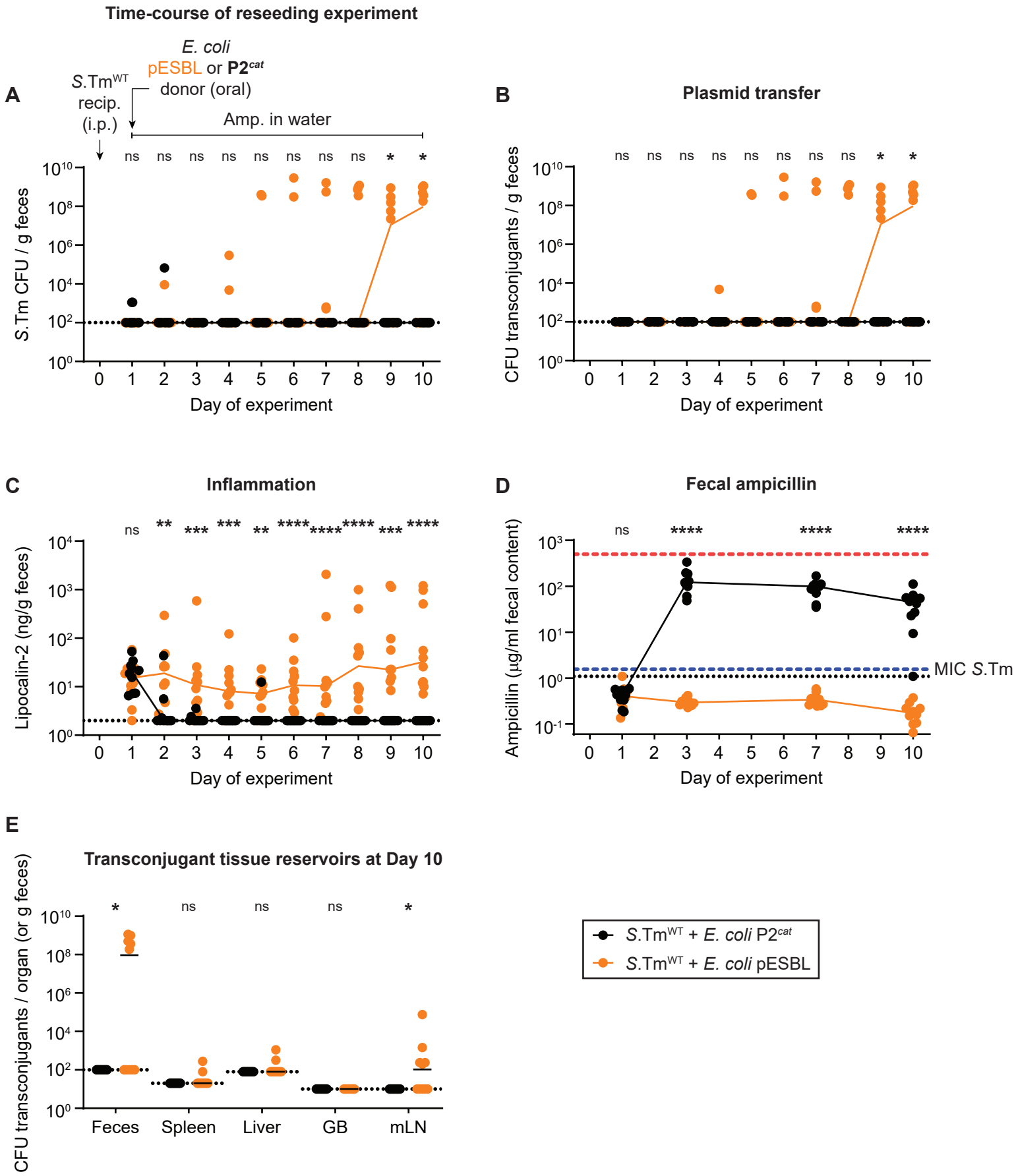

Bakkeren et al. Figure 4

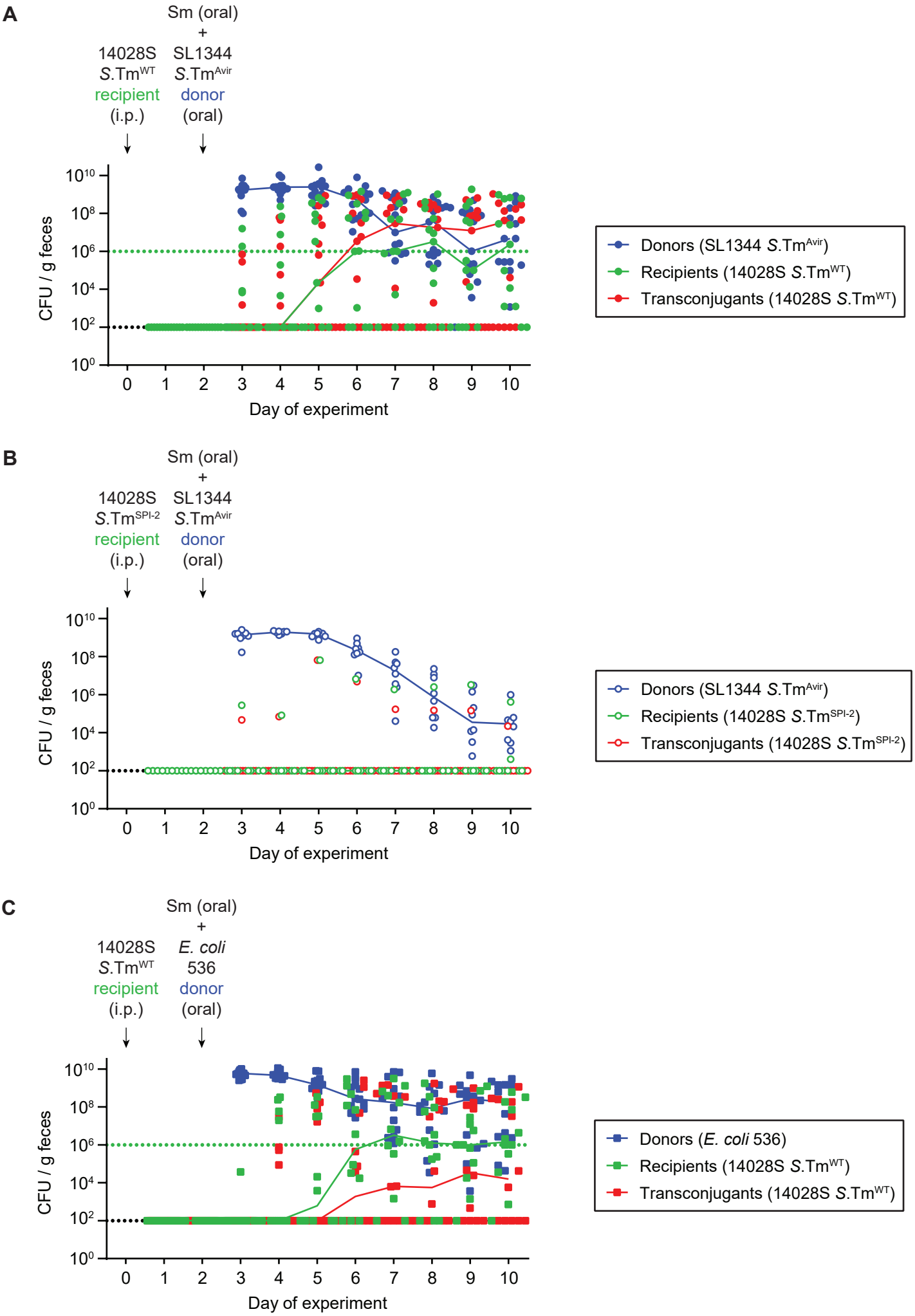

Bakkeren et al. Figure S1

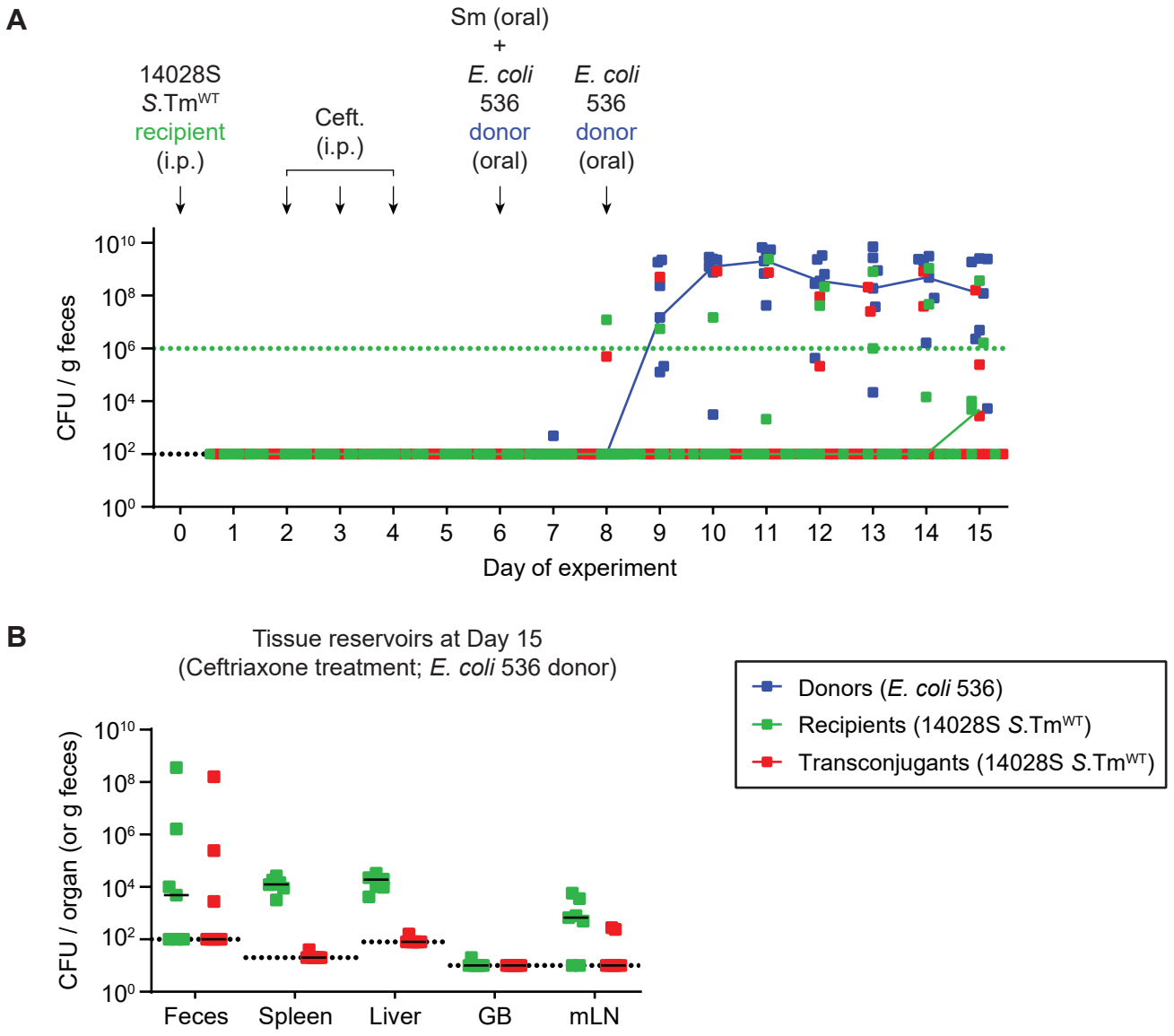

Bakkeren et al. Figure S2

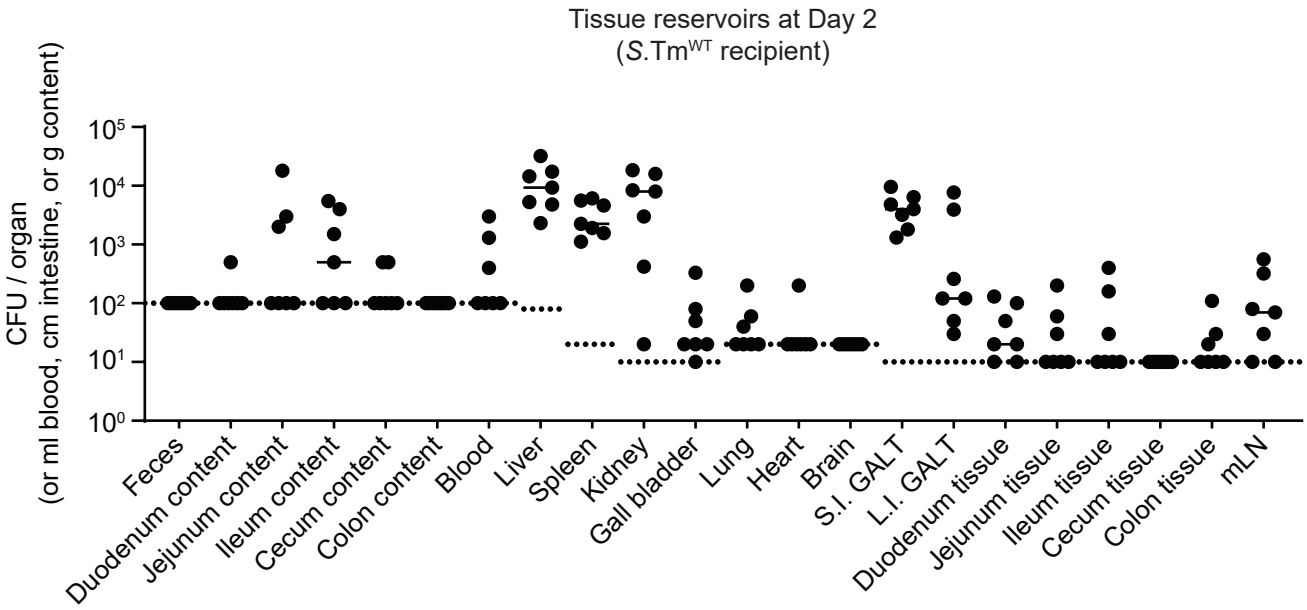

Bakkeren et al. Figure S3

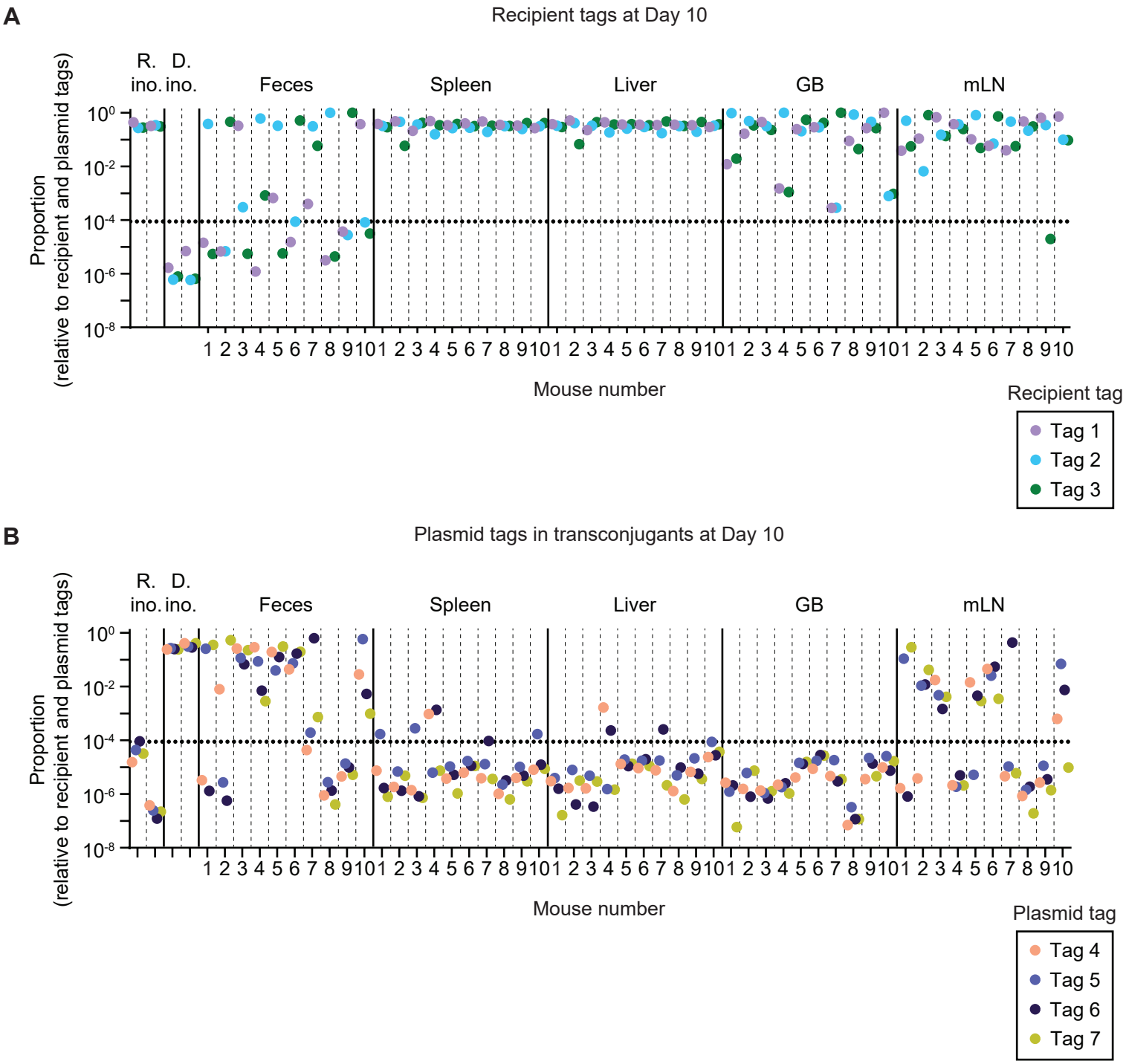

Bakkeren et al. Figure S4

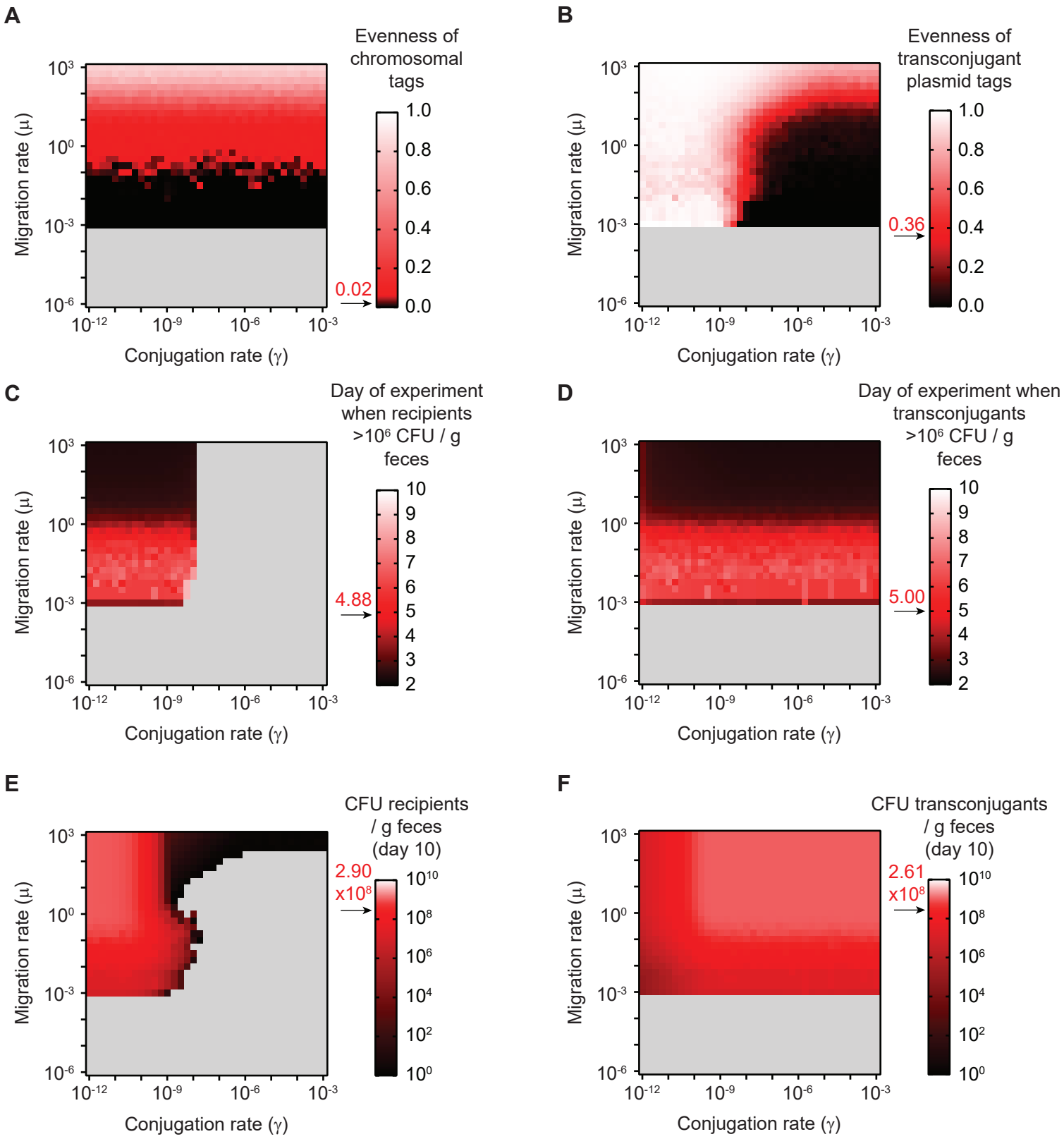

Bakkeren et al. Figure S5

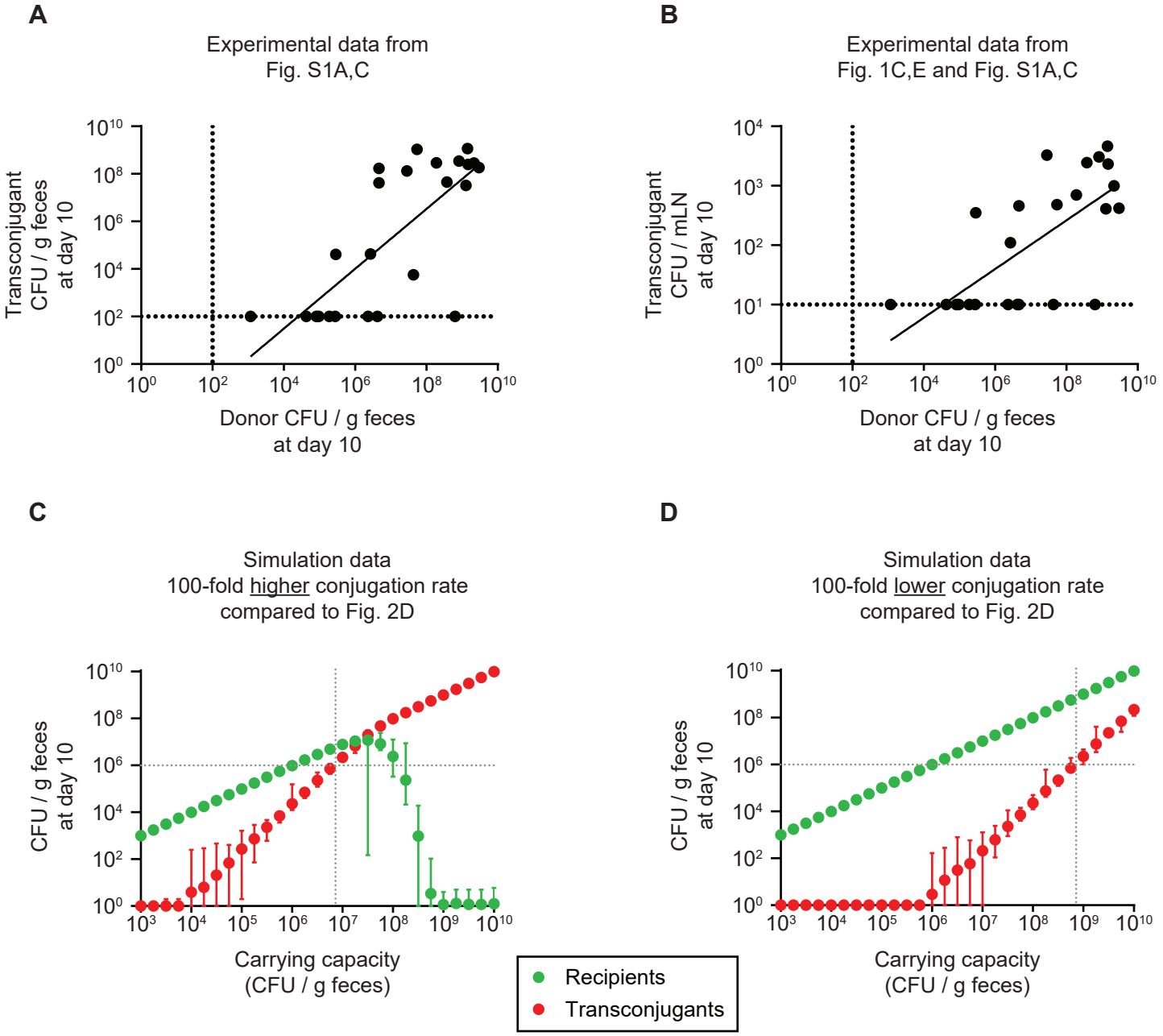

Bakkeren et al. Figure S6

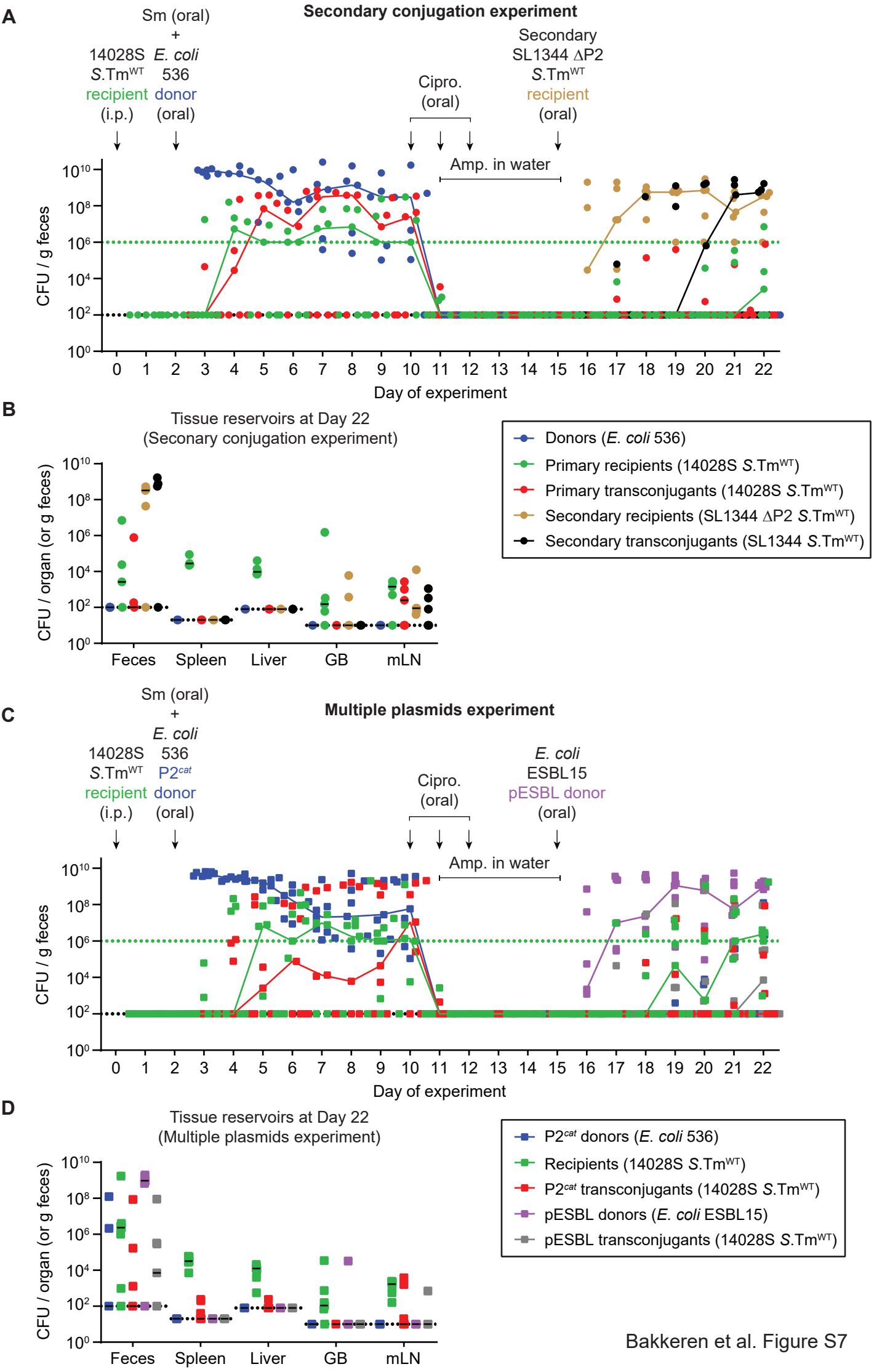

Bakkeren et al. Figure S7

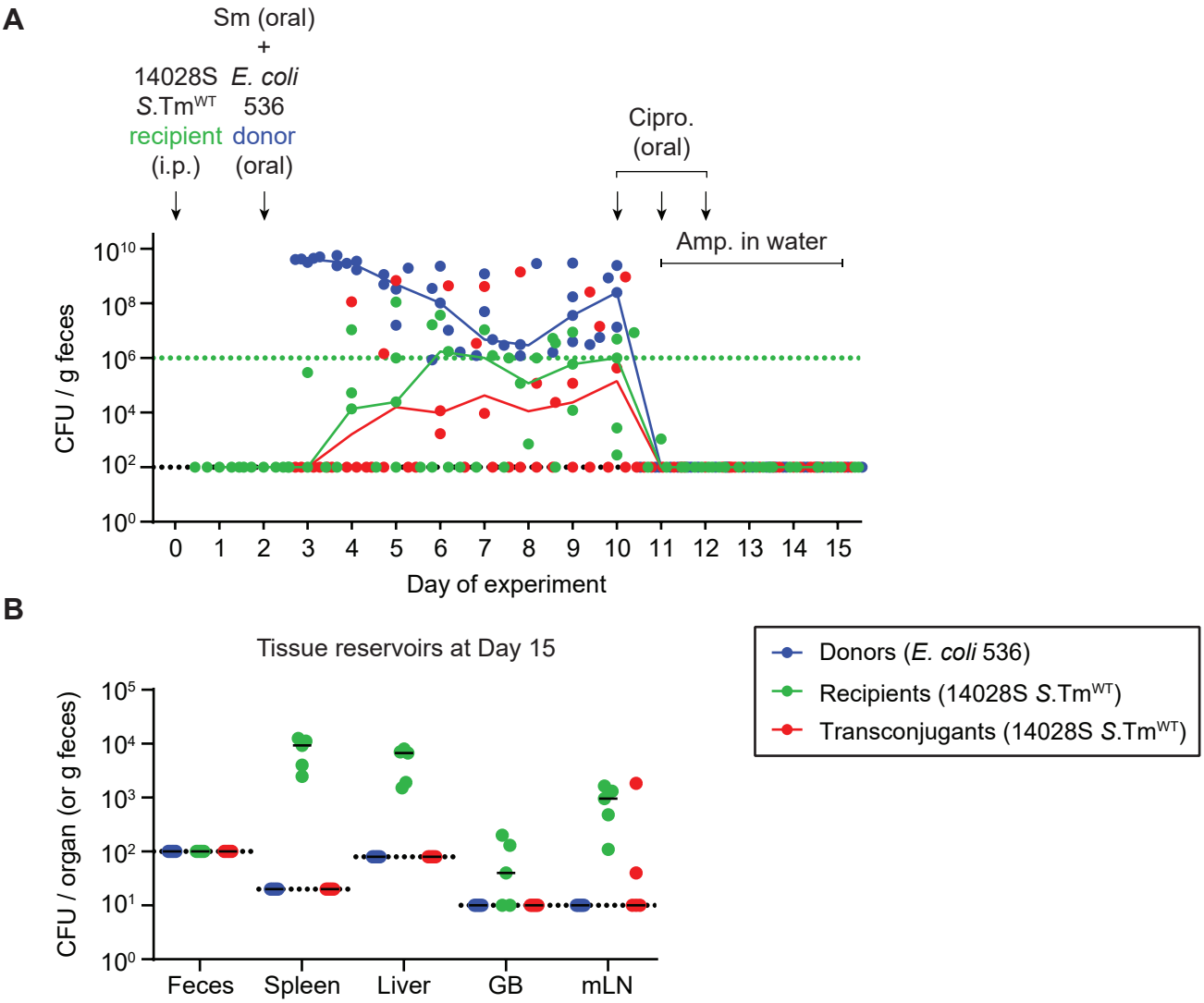

Bakkeren et al. Figure S8

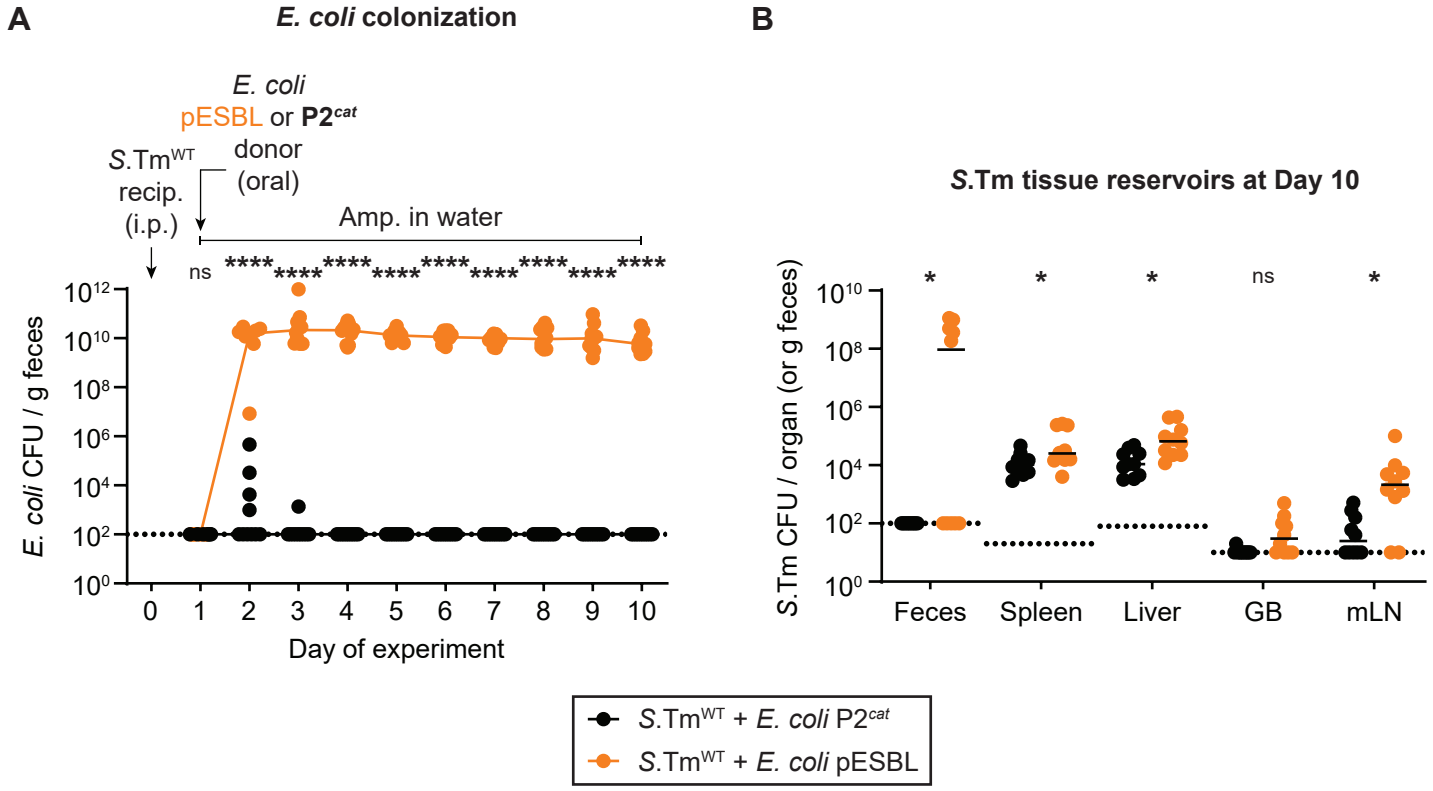

Bakkeren et al. Figure S9

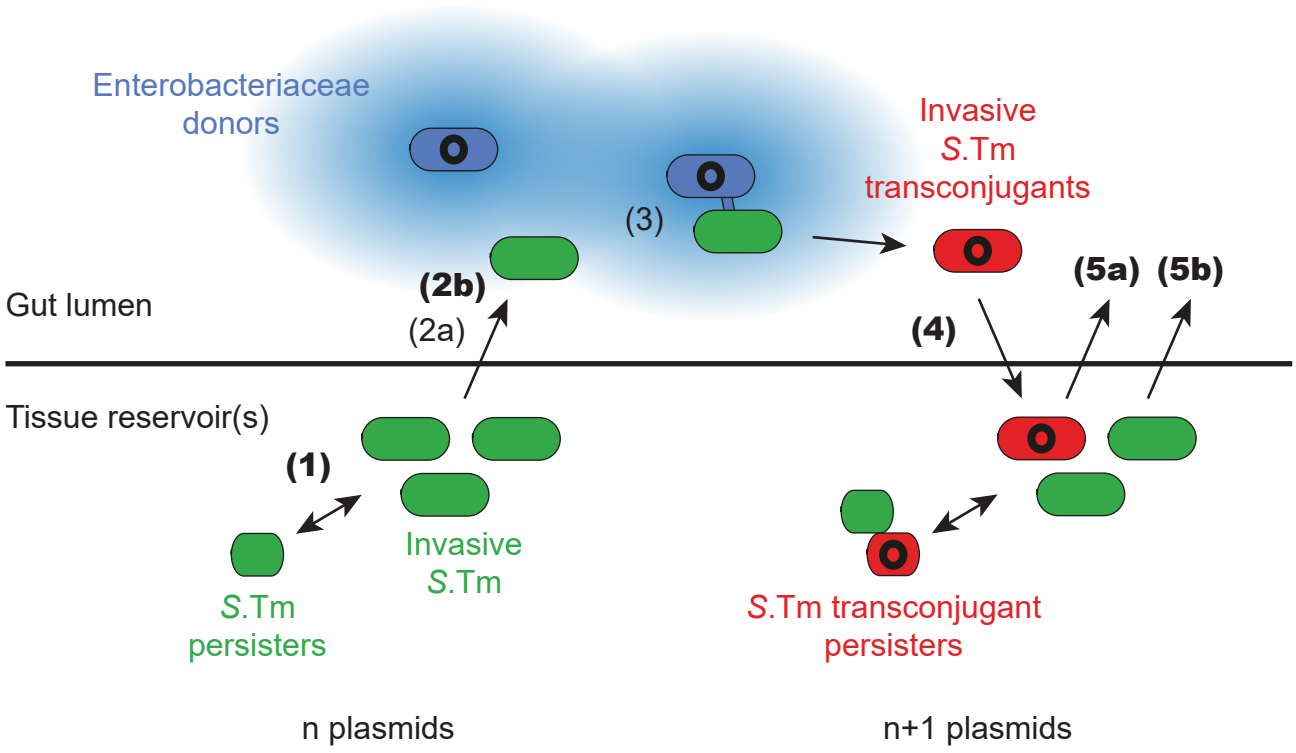

Bakkeren et al. Figure S10